공학박사학위논문

무선통신망에서 처리율 개선을 위한 신호전달 부하의 저감에 관한 연구

Signaling Overhead Reduction for Throughput Improvement in Wireless Networks

2014년 2월

서울대학교 대학원

전기·컴퓨터 공학부

이 동 헌

무선통신망에서 처리율 개선을 위한 신호전달 부하의 저감에 관한 연구

Signaling Overhead Reduction for Throughput Improvement in Wireless Networks

지도 교수 전 화 숙

이 논문을 공학박사 학위논문으로 제출함

2013년 12월

서울대학교 대학원

전기, 컴퓨터 공학부

이 동 헌

이동헌의 박사 학위논문을 인준함

2013년 12월

위 원 장 _____

부위원장 _____

위 원 _____

위 원 _____

위 원 _____

Abstract

Signaling Overhead Reduction for Throughput Improvement in Wireless Networks

Dong Heon Lee

The School of Electrical Engineering and Computer Science

The Graduate School

Seoul National University

Wireless networks usually adopt some link adaptation techniques to mitigate the performance degradation due to the time-varying characteristics of wireless channels. Since the link adaptation techniques require to estimate and collect channel state information, signaling overhead is inevitable in wireless networks. In this thesis, we propose two schemes to reduce the signaling overhead in wireless networks. First, we design an adaptive transmission scheme for cooperative communication networks. The cooperative network with the proposed scheme chooses the transmission rate and decides to involve the relay in transmission, adapting to the channel state estimated from limited feedback information (e.g., ACK/NACK feedback). Considering that the limited feedback information provides only partial knowledge about the actual channel states, we design a decision-making algorithm on cooperative transmission by using a partially observable Markov decision process (POMDP) framework. Next, we also propose a two-stage semi-distributed resource management framework for the device-to-device (D2D) communication in cellular networks. At the first stage of the framework, the base station (BS) allocates

resource blocks (RBs) to BS-to-user device (B2D) links and D2D links, in a centralized manner. At the second stage, the BS schedules the transmission using the RBs allocated to B2D links, while the primary user device of each D2D link carries out link adaptation on the RBs allocated to the D2D link, in a distributed fashion. The proposed framework has the advantages of both centralized and distributed design approaches, i.e., high network capacity and low signaling/computational overhead, respectively. We formulate the problems of RB allocation to maximize the radio resources efficiency, taking account of two different policies on the spatial reuse of RBs. To solve these problems, we suggest a greedy algorithm and a column generation-based algorithm. By simulation, it is shown that the proposed schemes achieve their design goal properly and outperform existing schemes while reducing the signaling overhead.

Keywords: Signaling overhead, cooperative communication, device-to-device communication, selection relaying, adaptive modulation and coding, resource management

Student Number: 2007-30232

Contents

List of Figures

List of Tables

Chapter 1. Introduction

1.1 Background and Motivation

Wireless networks suffer from the performance degradation due to the time-varying characteristics of a wireless channel. To mitigate this problem, wireless networks usually adopt some link adaptation techniques which adjust transmission parameters (e.g., transmission power, modulation and coding scheme (MCS) level, etc.) based on the current states of the wireless channels. These link adaptation techniques require to estimate and collect channel state information (CSI). Moreover, the information about which resources (e.g., time/frequency slots) are assigned to each user and the transmission parameters should be sent to the users. Therefore, signaling overhead is inevitable in wireless networks and reducing such signaling overhead is a fundamental research issue in wireless networks [1] – [3].

In this thesis, we focus on the signaling overhead problems in cooperative communication and in device-to-device (D2D) communication. Cooperative communication is one of promising technologies to mitigate channel impairments due to the time-varying characteristics of a wireless channel [4], [5]. In cooperative communication, one or more intermediate nodes between a source and its destination serve as relays to achieve spatial diversity by forwarding data from the source to the destination. To exploit variations in channel quality, some link adaptation techniques can be applied to cooperative communication. A representative adaptation technique is the adaptive modulation and coding (AMC) scheme where a MCS level is adjusted according to the channel state information (e.g., [6]). The selection relaying, which makes a relay forward data only when the signal strength at the relay exceeds a certain threshold (e.g., [7]), can also be considered as an adaptive coop-

erative scheme. Employing both the selection relaying and the AMC techniques, we can realize an adaptive cooperative communication scheme that fully benefits from channel variations. However, with multiple channels (i.e., source-destination, source-relay, and relay-destination channels) involved, the link adaptation in the cooperative communication incurs at least three times more signaling overhead (i.e., feedback overhead) compared to the link adaptation in an ordinary point-to-point channel. Moreover, intermittent participation of the relay due to the selection relaying technique forces the relay to send an extra signal for channel estimation.

To reduce such signaling overhead, many cooperative communication schemes under limited CSI has been proposed in [8] – [12]. The authors in [8] have proposed a practical incremental relaying scheme where the feedback from destination is not perfect. In [9], cooperative networks with the adaptive modulation have been investigated, assuming that the source-relay CSI is not available. An incremental relaying scheme with an implicit feedback from relays has been designed in [10]. The algorithm in [11] allocates the transmission time of the source and the relay based on the quantized channel feedback encoded into a small number of bits. The performance loss due to the quantization of the CSI in a cooperative network has been analyzed in [12]. Note that all these works have only focused on analyzing the performance of a simple cooperative communication scheme under limited CSI. However, to minimize the performance degradation, it is important to design an optimal decision-making algorithm which can fully take advantage of limited CSI. Therefore, we in this thesis propose adaptive transmission schemes with the optimal decision-making algorithm exploiting only limited CSI.

On the other hand, device-to-device (D2D) communication has gained much attention with an increasing demand for local data transmissions within a cell [13],

[14]. In D2D communication, a user equipment (UE) in a conventional cellular system can communicate with only the base station (BS). Dissimilarly to this BS-to-user device (B2D) communication, the D2D communication in cellular systems is defined as direct communication between UEs without passing through the BS. D2D communication enhances the spectral efficiency by spatially reusing radio resource and prolongs the battery life of UEs by reducing the transmission power. Due to these advantages, the D2D communication has been actively discussed in standardization bodies for the next-generation cellular systems such as Long-Term Evolution-Advanced (LTE-A) [15], [16]. In a cell of conventional cellular systems, a radio resource unit [e.g., a resource block (RB)] can be allocated to only one "cellular UE," which is a UE directly communicating with the BS via B2D link. However, in the cellular system using D2D communication, an RB can be spatially reused between B2D links and D2D links in a cell. Therefore, how well the resource management scheme supports the resource reuse by taking the intra-cell interference into account has a great influence on the overall network performance.

In orthogonal frequency division multiple access (OFDMA)-based cellular networks supporting D2D communications, the spatial reuse of radio resource has been pursued through power control [17], [18], interference coordination [19], [20], time hopping-based resource allocation [21], location-dependent resource allocation [22], link scheduling [23], mode selection [24], reusable resource selection for D2D links [25] – [27], graph theory-based resource allocation [28], joint scheduling and resource allocation [29], and a joint mode selection and resource allocation [30], [31]. They can be categorized largely into the centralized scheme (e.g., [18] – [22], [24] – [31]) and the distributed scheme (e.g., [17], [23]).

In the centralized scheme, the BS fully manages the resource not only for B2D links but also for D2D links. With a centralized scheme using the channel quality information (CQI) for all relevant links, the BS may optimally manage the resource. However, this strategy results in a substantial signaling overhead for reporting CQI. Moreover, a high computational burden falls on the BS since only the BS is in charge of managing resource.

On the other hand, in the distributed resource management scheme, the resource allocation for D2D communication is conducted by the UEs of each D2D link. Even though the distributed scheme reduces the signaling and computational overhead, due to the lack of overall CQI, its performance is usually worse than that of the centralized one. There have been only few studies on the distributed resource management. In [17], the authors focus on the case that just one cellular UE and one D2D link can be allocated to the same RBs. Ref. [23] provides a heuristic method to enable the simultaneous transmission of D2D links on the same resource. Therefore, in this thesis, we also propose a semi-distributed resource management framework for the D2D communication in OFDMA-based cellular networks, which aims at a high network throughput of centralized scheme and a low signaling/computational overhead of distributed one.

1.2 Approaches to Reduce Signaling Overhead

There have been so many works on the reduction of the signaling overhead in wireless networks. In this section, we will provide the overview of existing approaches to reduce the signaling overhead in wireless networks. The approaches used in the previous works can be categorized as follows: reducing the signaling information itself, controlling the interval of the signaling, grouping/clustering, and adopting a particular structure.

The first approach is to reduce the signaling information itself. The signaling information can be reduced by various ways. In [9], only the CSIs of a part of the relevant channels are used. The CSI is quantized into several bits in [11] and [12]. In [32], the source coding scheme that is used to compress the scheduling information of multiple users is proposed. In OFDMA systems, the best-M feedback, where each user reports the channel quality indicators on its M best RBs, is analyzed and optimized in [33]. In multiple-input multiple-output (MIMO) OFDM system, the differential codebook is proposed for the feedback information such as the number of data streams (i.e., rank) and the index of precoding matrix [34]. A CSI compression scheme using discrete cosine transform is proposed to reduce CSI feedback overhead [35].

The second approach is to controlling the interval of the signaling. The authors in [36] have investigated the optimization on the time interval of the uplink pilot for the channel estimation in order to overcome the impact of channel estimation error and delay on a TDD multiple-input single-output (MISO) beamforming system. In [37], the frame length for the downlink OFDMA systems are optimized to maximize the system efficiency by taking into account the amount of signaling overhead

needed to deliver the scheduling information to the users. The reporting mechanism that changes the reporting period of UE in an adaptive manner is proposed in [38].

The third approach is the grouping or clustering. The authors in [39] have proposed the group scheduling to reduce the signaling overhead in IEEE 802.16e system, where the mobile stations are clustered into multiple groups so that the resources are allocated to each group. In [40], the group-based control scheme is proposed for machine-type D2D communication where a large number of devices with small data transmissions are expected to communicate with each other by using D2D communication. In the scheme, since a group of links is a basic unit for resource allocation, the control overhead and computational complexity can be reduced.

The last approach is to adopt a particular structure. In [41], the semi-distributed resource management scheme is proposed for the relay-assisted cellular OFDMA networks. The BS first allocates resources to the directly connected mobile stations and relay stations. Then, RS allocates resources to the connected mobile stations. The authors in [42] adopts a two-stage scheme for the relay selection. At the first stage, a set of relays are selected based on the statistical channel quality information; at the second stage, the best relay within the set is selected based on instantaneous channel quality information.

In this thesis, we will propose two schemes as case studies of above-mentioned approaches. The first scheme adopts the first approach where only the CSIs of a part of the relevant channels are used. The second scheme belongs to the last approach because it adopts a semi-distributed control for the resource management. We will describe the proposed schemes in the following section.

1.3 Proposed Schemes

1.3.1 Adaptive Transmission Scheme for Cooperative Communication

To reduce the signaling overhead in the cooperative communication, we propose adaptive transmission schemes exploiting only limited CSI. First, we suggest a scheme that exchanges only the positive acknowledgement (ACK)/negative acknowledgement (NACK) feedback without any explicit CSI. The actual channel state can be inferred from the ACK/NACK feedback since an ACK (NACK) indicates a good (bad) channel state. In addition, we study the schemes where the CSI for a part (*not all*) of the relevant channels is fed back to more accurately infer the channel state.

While these schemes can reduce signaling overhead, overall performance can be degraded because of insufficient channel information. On the basis of only limited CSI, these schemes should decide the MCS level (for the AMC technique) as well as whether the relay forwards data or not (for the selection relaying technique) every frame. Since the adaptive transmission scheme relies only on partial information about the channel states from limited CSI, the decision-making problem in this scenario fits well with the partially observable Markov decision process (POMDP) model [43]. Therefore, we design the decision-making algorithm by using the POMDP framework. By simulation, we show that the proposed scheme with the optimal decision-making algorithm minimizes the performance degradation caused by lack of information and, as a result, outperforms the adaptive cooperative communication scheme with the full feedback by reducing signaling overhead.

1.3.2 Resource Management Scheme for D2D Communication in Cellular Networks

To reduce the signaling overhead in the D2D communication, we also propose a semi-distributed resource management framework for the D2D communication in OFDMA-based cellular networks, which aims at a high network throughput of centralized scheme and a low signaling/computational overhead of distributed one. Specifically, the proposed scheme adopts a two-stage resource management strategy. In the first stage, the BS allocates RBs to B2D and D2D links, based on the limited channel information which is not an accurate channel gain but the path loss of all relevant links. In the second stage, the UEs of each D2D link decide the MCS level and the transmission power for the link, while the BS schedules the transmission to/from each cellular UE on the corresponding B2D link. It is noted that the first and second stage operations are invoked on a long-term basis and a short-term basis, respectively.

Our specific concern is to design efficient RB allocation schemes. We consider two policies on the spatial reuse of RBs. With the first policy, multiple D2D links can coexist on the same RB, but they are not allowed to share an RB with any B2D link. The performance gain of this policy comes from the RB reuse just between D2D links. We formulate an optimization problem of RB allocation with this policy to maximize the spatial reuse of RBs by multiple D2D links. To solve the problem, we convert the problem into a well-known multiple set covering problem and present a greedy algorithm for obtaining the solution. The second policy is that a B2D link and multiple D2D links can be scheduled together in the same RBs. With this policy, we formulate another RB allocation problem to maximize the minimum

of the expected number of RBs allocated to each B2D link. Then, we solve the problem by converting it into a linear programming (LP) problem. Since the LP problem has a very large number of variables, we adopt the column generation approach by which the problem is effectively solved with a lower computational complexity.

From a viewpoint of resource allocation, the previous works [24] – [31] have some limitations, compared to our schemes. The authors in [24], [25], [27] and [29] have focused on the case that just one B2D link and one D2D link can share the same resource, without consideration of the spatial reuse between D2D links. In [31], each subchannel can be assigned to at most one link (i.e., B2D or D2D link) in a time slot. Similarly to our work, the schemes in [26], [28], and [30] allow the coexistence of one B2D link and multiple D2D links on the same resource. However, in [26], the authors have taken a heuristic approach to design a resource allocation scheme. The authors in [28] have designed a resource allocation scheme to maximize the network sum-rate without considering QoS requirements of links. Although the authors in [30] have formulated an optimization problem in consideration of the interference between links, they have eventually ignored the interference in solving the problem. Therefore, none of the aforementioned works has attempted to design a practical resource management scheme using the optimization approach under the two-stage semi-distributed resource management framework to reduce the signaling/computational overhead.

1.4 Organization

The remainder of the thesis is organized as follows. Chapter 2 explains the adaptive transmission scheme for cooperative communication. Section 2.1 presents the system model and Section 2.2 describes operation of the proposed network. In Section 2.3, we design an adaptive transmission scheme by using the POMDP framework.

In Chapter 3, we describe the resource management scheme for D2D communication in cellular networks. Section 3.1 describes the system model. A two-stage semi-distributed resource management framework is suggested in Section 3.2. We investigate in Section 3.3 the conditions for simultaneous transmission of B2D links and D2D links. Based on simultaneous transmission conditions, Section 3.4 formulates the optimization problems and presents the algorithms to solve the problems.

In Chapter 4, we present the simulation results of two schemes. In Section 4.1, we show the performance of the adaptive transmission scheme for cooperative communication with numerical results. Section 4.2 presents the simulation results of the resource management scheme for D2D communication in cellular networks. Finally, the thesis is concluded with Chapter 5.

Chapter 2. Adaptive Transmission Scheme for Cooperative Communication

In this chapter, we propose an adaptive transmission scheme for cooperative communication networks. The proposed scheme adaptively selects the MCS level as well as whether the relay forwards data or not every frame based only on limited CSI (i.e., the CSI for a part of the relevant channels). Since the POMDP framework permits the uncertainty of information in modeling the decision making problem, we design the proposed scheme by using the POMDP framework.

2.1 System Model

We consider a cooperative transmission system which consists of three nodes: a source (S), a relay (R), and a destination (D). This three-node cooperative network can be viewed as a small-scale network such as a wireless local area network (WLAN) or a basic building block of a larger wireless network. We assume that the relay is preselected and is dedicated for the transmission of the source-destination pair.

In this network, three wireless channels are involved: a source-destination (SD) channel, a source-relay (SR) channel, and a relay-destination (RD) channel. The channel fading gains of the SD, SR, and RD channels are denoted by $g^{(SD)}$, $g^{(SR)}$, and $g^{(RD)}$, respectively. The time is divided into frames of fixed duration T_F. We assume that the channels are independent of each other and the channel fading gains remain constant during a frame (i.e., block fading channel). The network operates on a frequency band with the bandwidth of W. The source and the relay transmit with power ρ.

In each frame, the source transmits one packet which consists of multiple symbols to the destination. The MCS level of a packet is adjusted by using the AMC technique. Either the source can transmit a packet directly to the destination or the relay can assist the transmission of the packet. At the beginning of each frame (a *decision epoch*), the source decides the MCS level as well as the relay participation for the frame. To notify the relay and the destination of the decision, the source includes the decision in the packet header.

Let us explain the AMC technique in detail. The MCS level of the packet for the tth frame is denoted by L_t. The MCS level is selected among K different levels, that is, $L_t \in \{1, 2, \ldots, K\}$. When the MCS level l is chosen, the number of bits per symbol b_l is determined according to the chosen modulation level. Also, code rate c_l, which is the number of information bits per transmitted symbol, is determined. Then, if a packet with B symbols is transmitted in a frame, the transmission rate $r_l(B)$ is calculated as $r_l(B) = b_l c_l B/T_F$.

The relay participation for the tth frame is denoted by $Y_t \in \{0, 1\}$. If $Y_t = 0$, the relay does not participate in the transmission in the tth frame (i.e., direct transmission). When $Y_t = 1$, the relay forwards a received packet to the destination in the tth frame.

2.2 Cooperative Networks with Limited Feedback

2.2.1 Operation of the Proposed Cooperative Network

Fig. 2.1 illustrates an operation example of the proposed cooperative network. In the tth frame in which the relay participation is decided as $Y_t = y$, the number of symbols in a packet is B_y and the transmission time of a packet is T_y. If the

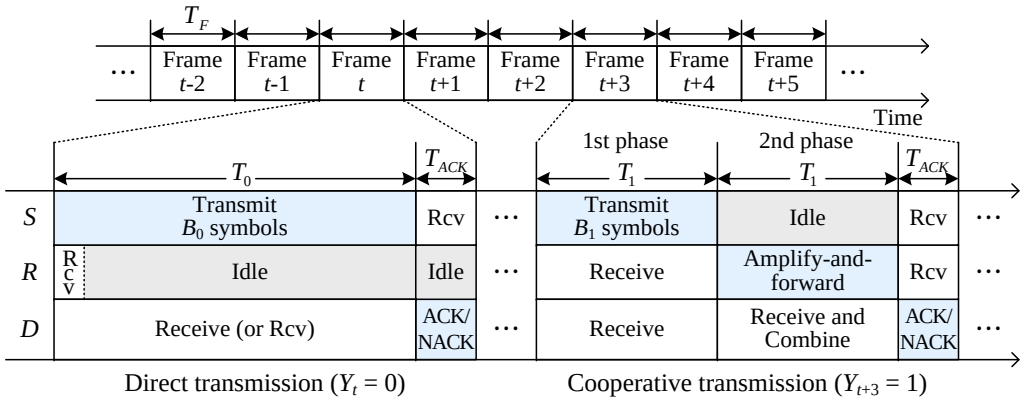

Fig. 2.1: Operation example of the proposed cooperative network.

source decides the direct transmission [see the frame t in Fig. 2.1], a packet with B_0 symbols using the chosen MCS level L_t is transmitted during the period T_0. The received signal at the destination, denoted by θ^D, is expressed as[1]

$$\theta^D[n] = g^{(SD)}x[n] + \zeta, \qquad \text{for } n = 1, 2, \ldots, B_0, \tag{2.1}$$

where n is the symbol index and ζ is the additive white Gaussian noise which has a constant noise spectral density of N_0. In this case, the signal-to-noise radio (SNR) of the packet is simply the SNR of the SD channel, which is $\gamma^{(SD)} = g^{(SD)}\rho/(N_0 W)$.

If the source decides the cooperative transmission [see the frame t+3 in Fig. 2.1], the frame consists of two transmission phases. In the first phase, the source transmits a packet with B_1 symbols to both the relay and the destination during the period T_1.[2] The received signals at the relay and the destination in the first phase

[1]For simplicity of description, the frame index t is omitted.

[2]As shown in Fig. 2.1, since the duration of T_1 is about half of that of T_0, the number of symbols B_1 is also about half of B_0.

can be written as, respectively,

$$\theta_1^R[n] = g^{(SR)}x[n] + \zeta, \qquad \text{for } n = 1, 2, \ldots, B_1, \tag{2.2}$$

$$\theta_1^D[n] = g^{(SD)}x[n] + \zeta, \qquad \text{for } n = 1, 2, \ldots, B_1. \tag{2.3}$$

We consider the amplify-and-forward (AF) as the relaying strategy. Therefore, in the second phase, the relay simply amplifies the received packet by a factor of G, and forwards it to the destination. Then, the received signal at the destination in the second phase is

$$\theta_2^D[n] = g^{(RD)}G\theta_1^R[n] + \zeta, \qquad \text{for } n = 1, 2, \ldots, B_1, \tag{2.4}$$

According to [7], we choose $G = \sqrt{\rho/(g^{(SR)}\rho + N_0W)}$. The packets received in the first phase and the second phase are combined at the destination by using the maximal-ratio combining (MRC). The SNR of the packet after combining is given in [7] by

$$\gamma_c = \gamma^{(SD)} + \frac{\gamma^{(SR)}\gamma^{(RD)}}{\gamma^{(SR)} + \gamma^{(RD)} + 1} \tag{2.5}$$

where $\gamma^{(SR)} = \frac{g^{(SR)}\rho}{(N_0W)}$ and $\gamma^{(RD)} = \frac{g^{(RD)}\rho}{(N_0W)}$ are the SNRs of the SR and RD channels, respectively.

At the end of each frame, if the destination correctly receives the packet, it transmits an ACK packet to the source during the period T_{ACK}. Accordingly, the source transmits the next packet in the next frame. Otherwise, the destination discards the packet and transmits a NACK packet to the source for requesting the retransmission of the same packet. Let η_t denote an ACK/NACK indicator in the tth frame: if the ACK packet is returned, $\eta_t = 1$; otherwise, $\eta_t = 0$. The ACK/NACK packet is assumed to be error-free. All packet transmissions are separated by a short constant time spacing, irrespective of packet type.

2.2.2 Finite-State Markov Channel Model

As mentioned above, the proposed network involves three wireless channels of SD, SR, and RD channels. Each channel is assumed to be subject to Rayleigh fading. We model a Rayleigh fading channel as finite state Markov channel (FSMC), where the received instantaneous SNR is partitioned into M non-overlapping intervals (i.e., M states). In [44], it is shown that the FSMC model well represents the time-varying behavior of a Rayleigh fading channel.

Let $\mathbf{\Gamma}^{(\xi)} = \{\Gamma_1^{(\xi)}, \Gamma_2^{(\xi)}, \cdots, \Gamma_{M+1}^{(\xi)}\}$ denote the thresholds of the received SNR for channel ξ in increasing order with $\Gamma_1^{(\xi)} = 0$ and $\Gamma_{M+1}^{(\xi)} = \infty$, for $\xi \in \{SD, SR, RD\}$. Hereafter, the superscript (ξ) means "for channel ξ." Then, the channel ξ is said to be in state $i \in \{1, 2, \cdots, M\}$, if the SNR of the channel is in the range $[\Gamma_i^{(\xi)}, \Gamma_{i+1}^{(\xi)})$. When $s_t^{(\xi)}$ denotes the state of channel ξ at the tth decision epoch, we have $s_t^{(\xi)} = i$, if $\Gamma_i^{(\xi)} \leq \gamma^{(\xi)} < \Gamma_{i+1}^{(\xi)}$. Let $p_{i,j}^{(\xi)} := \Pr\{s_{t+1}^{(\xi)} = j \mid s_t^{(\xi)} = i\}$ denote the transition probability from state i to state j of channel ξ. We assume that the Rayleigh fading is slow enough that the transition occurs only into neighboring states, i.e., $p_{i,j}^{(\xi)} = 0, \forall |i - j| > 1$. Then, the transition probabilities can be approximated in [44] as follows.

The steady-state probability of state i is given by

$$\Omega_i^{(\xi)} := \Pr\{s_t^{(\xi)} = i\} = \int_{\Gamma_i^{(\xi)}}^{\Gamma_{i+1}^{(\xi)}} e^{-\gamma} \mathrm{d}\gamma, \qquad \text{for } i = 1, 2, \ldots, M. \tag{2.6}$$

Let $\overline{\gamma^{(\xi)}}$ denote the average SNR and $f_d^{(\xi)}$ denote the maximum Doppler frequency defined as the ratio of the speed of the mobile node to the wavelength. Then, the

transition probabilities can be approximated in [44] as

$$p_{i,i+1}^{(\xi)} = N^{(\xi)}(\Gamma_{i+1}^{(\xi)}) \times T_F/\Omega_i^{(\xi)}, \qquad \text{for } i = 1, 2, \ldots, M-1, \tag{2.7}$$

$$p_{i,i-1}^{(\xi)} = N^{(\xi)}(\Gamma_{i}^{(\xi)}) \times T_F/\Omega_i^{(\xi)}, \qquad \text{for } i = 2, 3, \ldots, M, \tag{2.8}$$

where $N^{(\xi)}(\cdot)$ is the expected number of level crossings given as

$$N^{(\xi)}(\Gamma) = \sqrt{2\pi\Gamma/\,\overline{\gamma^{(\xi)}}} \times f_d^{(\xi)} \times e^{\left(-\Gamma/\overline{\gamma^{(\xi)}}\right)}. \tag{2.9}$$

Once the average SNR and the maximum Doppler frequency are known, the state transition probabilities are determined according to above equations. The transition probabilities can be also calculated by a Monte Carlo simulation from Jakes' model [45].

2.2.3 Packet Error Probability

The packet error probability in the tth frame depends on the received SNRs of all channels $\boldsymbol{\gamma} = (\gamma^{(SD)}, \gamma^{(SR)}, \gamma^{(RD)})$, the MCS level l, and the relay participation y. For a given $(\boldsymbol{\gamma}, l, y)$, we will calculate the packet error probability which is denoted by $\psi_{\text{pkt}}(\boldsymbol{\gamma}, l, y)$. In this thesis, to calculate the packet error probability, we adopt the approach used in [46]. We consider the μ-ary quadrature amplitude modulation (μ-QAM) scheme. The SNR per symbol, denoted by γ, is calculated as $\gamma = E_{\text{S}}/N_0$, where E_{S} is the signal energy per symbol. In the μ-QAM modulation with coherent detection and Gray coding, for a given value of γ, the approximated bit error probability is given in [47] by

$$\psi_{\text{b}}(\mu, \gamma) \approx \frac{4}{\log_2 \mu} Q\Big(\sqrt{\frac{3\gamma \log_2 \mu}{\mu - 1}}\Big) \tag{2.10}$$

where $Q(x)$ is the Q-function, i.e., $Q(x) = (1/\sqrt{2\pi}) \int_x^\infty e^{-t^2/2} dt$.

We assume that a packet consists of z forward error correction (FEC) blocks each of which is encoded by the Reed-Solomon (RS) code. An (n, m) RS code block consists of n code symbols that can correct up to $\lfloor \frac{n-m}{2} \rfloor$ code symbol errors, where $\lfloor x \rfloor$ is the largest integer smaller than or equal to x. In practice, it is common to use the RS code with $n = 2^\alpha - 1$ where α is an arbitrary positive integer. In this case, each code symbol is composed of α bits. Then, the code symbol error probability ψ_{sym} is the probability that at least one bit error occurs in the code symbol, i.e.,

$$\psi_{\text{sym}} = 1 - (1 - \psi_{\text{b}})^{\log_2(n+1)}. \tag{2.11}$$

The error probability of an (n, m) RS code block is the probability that more than $\lfloor \frac{n-m}{2} \rfloor$ code symbol errors occur in a code block. That is,

$$\psi_{\text{block}} = 1 - \sum_{m'=0}^{\lfloor \frac{n-m}{2} \rfloor} \binom{n}{m'} (\psi_{\text{sym}})^{m'} (1 - \psi_{\text{sym}})^{n-m'}. \tag{2.12}$$

Then, the packet error probability of the packet is calculated as

$$\psi_{\text{pkt}} = 1 - (1 - \psi_{\text{block}})^z. \tag{2.13}$$

For the FSMC model, when the MCS level is l, the relay participation is y, and the SD, SR, and RD channels are respectively in the state i, j, and k, the packet error probability is $\psi_{\text{pkt}}(\boldsymbol{\gamma}_{(i,j,k)}, l, y)$ where

$$\boldsymbol{\gamma}_{(i,j,k)} = \Big(\frac{\Gamma_i^{(SD)} + \Gamma_{i+1}^{(SD)}}{2}, \frac{\Gamma_j^{(SR)} + \Gamma_{j+1}^{(SR)}}{2}, \frac{\Gamma_k^{(RD)} + \Gamma_{k+1}^{(RD)}}{2} \Big) \tag{2.14}$$

Hereafter, we will use $\chi_{(i,j,k)}^{(l,y)}$ as another short notation for $\psi_{\text{pkt}}(\boldsymbol{\gamma}_{(i,j,k)}, l, y)$.

2.2.4 Channel Feedback Schemes

To reduce the feedback overhead, the proposed scheme decides the MCS level and the relay participation based only on limited CSI. Essentially, the source can infer the channel state from the ACK/NACK packet without any explicit feedback since receiving the ACK (NACK) packet means a good (bad) channel state. To infer the channel state more accurately, additional information can be piggybacked on the ACK/NACK packet. We consider three different feedback schemes according to the amount of feedback overhead as follows:

- **ACK/NACK only:** No additional information is piggybacked on the ACK/NACK packet. Thus, the source only receives the ACK/NACK indicator η_t as feedback in the tth frame.
- **One-CSI feedback:** The state of SD channel, i.e., $s_t^{(SD)}$, is piggybacked on the ACK/NACK packet in the tth frame.
- **Two-CSI feedback:** The states of the SD and RD channels, i.e., $s_t^{(SD)}$ and $s_t^{(RD)}$, are piggybacked on the ACK/NACK packet in the tth frame. In the case of direct transmission, only $s_t^{(SD)}$ is piggybacked since $s_t^{(RD)}$ cannot be estimated by the destination.

2.3 Adaptive Transmission Scheme for Cooperative Communication

2.3.1 POMDP Formulation

Since the source does not have exact knowledge of the state of each channel, at the tth decision epoch, it should decide L_t and Y_t based on all information available to the source up until the $(t-1)$th frame, in order to make a decision. The available information includes the history of the MCS level and the relay participation until the $(t-1)$th frame, i.e., L_i and Y_i for $i = 1, \ldots, t-1$, as well as the history of the channel feedback, i.e., η_i for $i = 1, \ldots, t-1$ (ACK/NACK only feedback), $(\eta_i, s_i^{(SD)})$ for $i = 1, \ldots, t-1$ (one-CSI feedback), or $(\eta_i, s_i^{(SD)}, s_i^{(RD)})$ for $i = 1, \ldots, t-1$ (two-CSI feedback). This decision making problem fits very well with the POMDP framework which permits the uncertainty of information in modeling the decision making problem [43]. Under the POMDP model, the source can estimate the state of each channel and decide L_t and Y_t from which it can obtain the highest reward for these estimated channel states. Therefore, we model the decision-making problem as a POMDP.

A POMDP problem consists of six elements: a state space, an action space, a transition probability, an observation space, an observation probability, and a reward. We now define each element one by one. One can refer to [43] for more information of the POMDP model.

State

The state at the tth decision epoch is represented by $\boldsymbol{s}_t = \left(s_t^{(SD)}, s_t^{(SR)}, s_t^{(RD)}\right)$, where $s_t^{(\xi)} \in \{1, 2, \ldots, M\}$ is the state of channel ξ at the tth decision epoch, for $\xi \in \{SD, SR, RD\}$.

Action

Let $A_t = (L_t, Y_t)$ denote the action selected at the tth decision epoch where $L_t \in \{1, 2, \ldots, K\}$ is the MCS level and $Y_t \in \{0, 1\}$ is the relay participation.

State Transition Probability

In our model, the state transition of a channel is independent of the chosen action. Thus, after tth decision epoch, the channel state changes from the state $\boldsymbol{s}_t = (i, j, k)$ to the state $\boldsymbol{s}_{t+1} = (i', j', k')$, according to the state transition probability $p_{(i,j,k)(i',j',k')} := \Pr\{\boldsymbol{s}_{t+1} = (i', j', k') \mid \boldsymbol{s}_t = (i, j, k)\}$. Furthermore, based on the assumptions in Section 2.1, the transition probabilities of the SD, SR, and RD channels modelled by FSMC are independent of each other. That is,

$$p_{(i,j,k)(i',j',k')} = p_{i,i'}^{(SD)} \times p_{j,j'}^{(SR)} \times p_{k,k'}^{(RD)} \tag{2.15}$$

where $p_{v,w}^{(\xi)}$ is the transition probability of channel ξ from state v to state w.

Observation

Let O_t denote the observation that the source obtains after the tth decision epoch. Also, we define $q_{(i,j,k),o}^{a}$ as the observation probability that the source obtains the observation o in the state (i, j, k) when the action $a = (l, y)$ is taken. That is,

$q^a_{(i,j,k),o} := \Pr\{O_t = o \mid \boldsymbol{s}_{t+1} = (i,j,k), A_t = a\}$. According to the adopted feedback scheme, the observation and the observation probability are defined as follows:

- **ACK/NACK only:** The success or failure of the transmission of a packet is the observation, i.e., $O_t = \eta_t$, where η_t is the ACK/NACK indicator: if the ACK packet is returned, $\eta_t = 1$; otherwise, $\eta_t = 0$. Then, we get $q^a_{(i,j,k),1} = 1 - \chi^a_{(i,j,k)}$ and $q^a_{(i,j,k),0} = \chi^a_{(i,j,k)}$, where $\chi^a_{(i,j,k)}$ is the packet error probability.

- **One-CSI feedback:** The SD channel state as well as the success or failure of a transmitted packet constitutes the observation, i.e., $O_t = \left(\eta_t, s_t^{(SD)}\right)$. If we define $o = (o^{(1)}, o^{(2)})$, we get $q^a_{(i,j,k),(1,i)} = 1 - \chi^a_{(i,j,k)}$ and $q^a_{(i,j,k),(0,i)} = \chi^a_{(i,j,k)}$. Also, we get $q^a_{(i,j,k),(o^{(1)},o^{(2)})} = 0$ for all o such that $o^{(2)} \neq i$.

- **Two-CSI feedback:** The success or failure of a transmitted packet, the SD channel state, and the RD channel state constitute the observation. Let $o = (o^{(1)}, o^{(2)}, o^{(3)})$. We first examine the direct transmission. If the source chooses the direct transmission, the RD channel state is marked as zero since the RD channel state cannot be estimated. Therefore, in the case of direct transmission ($y = 0$), $O_t = \left(\eta_t, s_t^{(SD)}, 0\right)$. Then, we get $q^{(l,0)}_{(i,j,k),(1,i,0)} = 1 - \chi^{(l,0)}_{(i,j,k)}$ and $q^{(l,0)}_{(i,j,k),(0,i,0)} = \chi^{(l,0)}_{(i,j,k)}$. Also, we get $q^{(l,0)}_{(i,j,k),(o^{(1)},o^{(2)},o^{(3)})} = 0$ for all o such that $o^{(2)} \neq i$ or $o^{(3)} \neq 0$. On the other hand, in the case of cooperative transmission ($y = 1$), we have $O_t = \left(\eta_t, s_t^{(SD)}, s_t^{(RD)}\right)$. Then, we get $q^{(l,1)}_{(i,j,k),(1,i,k)} = 1 - \chi^{(l,1)}_{(i,j,k)}$ and $q^{(l,1)}_{(i,j,k),(0,i,k)} = \chi^{(l,1)}_{(i,j,k)}$. Also, we get $q^{(l,1)}_{(i,j,k),(o^{(1)},o^{(2)},o^{(3)})} = 0$ for all o such that $o^{(2)} \neq i$ or $o^{(3)} \neq k$.

Reward

Let $R^a_{(i,j,k)}$ denote the instantaneous reward when the action a is taken in the state (i,j,k). The objective of the decision-making algorithm is to maximize the average throughput. Thus, it is obvious that the instantaneous reward is the expected throughput gain. That is, $R^a_{(i,j,k)} = r_l(B_y) \times \left(1 - \chi^a_{(i,j,k)}\right)$, where $r_l(B_y)$ is the transmission rate when the action $a = (l,y)$ is chosen.

2.3.2 Solution to POMDP

To choose a proper action, the source maintains the "belief vector" which contains all the necessary information for making an optimal decision [43]. The belief vector at the tth decision epoch is denoted by

$$\boldsymbol{\pi}(t) = \left(\pi_{(i,j,k)}(t)\right)_{i,j,k=1,2,\ldots,M} \tag{2.16}$$

where $\pi_{(i,j,k)}(t)$ is the probability of the state (i,j,k) at the tth decision epoch. At the network initialization, since the source does not have any information about the channel state, the initial probability $\pi_{(i,j,k)}(1)$ is assumed to be $\Omega_i^{(SD)} \times \Omega_j^{(SR)} \times \Omega_k^{(RD)}$, where $\Omega_v^{(\xi)}$ is the steady-state probability of state v for channel ξ. After the tth decision epoch, the source updates $\boldsymbol{\pi}(t+1)$ based on $\boldsymbol{\pi}(t)$, the action, and the observation by Bayes' theorem. When $T_{(i,j,k)}(\boldsymbol{\pi}(t), a, o) := \Pr\{\boldsymbol{s}_{t+1} = (i,j,k) \mid$

$\boldsymbol{\pi}(t), A_t = a, O_t = o\}$,

$$\pi_{(i,j,k)}(t+1) = T_{(i,j,k)}(\boldsymbol{\pi}(t), a, o)$$
$$= \frac{q^a_{(i,j,k),o} \sum_{l=1}^{M}\sum_{m=1}^{M}\sum_{n=1}^{M} p_{(l,m,n)(i,j,k)}\pi_{(l,m,n)}(t)}{\sum_{i'=1}^{M}\sum_{j'=1}^{M}\sum_{k'=1}^{M}\Big(q^a_{(i',j',k'),o}\sum_{l=1}^{M}\sum_{m=1}^{M}\sum_{n=1}^{M} p_{(l,m,n)(i',j',k')}\pi_{(l,m,n)}(t)\Big)}. \tag{2.17}$$

The policy δ is a mapping function from the belief vector to an action. At the tth decision epoch, the source chooses $\delta\big(\boldsymbol{\pi}(t)\big)$ as an action. Among all the possible policies, the optimal policy δ^* is the one that maximizes the objective function which is the expected discounted reward in an infinite horizon with discount factor κ $(0 < \kappa < 1)$. Solving the POMDP is equivalent to finding this optimal policy δ^*.

For finding the optimal policy, we define $U^*_a(\boldsymbol{\pi})$ which represents the maximum expected reward of the action a when the current belief vector is $\boldsymbol{\pi}$. That is,

$$\begin{aligned} U^*_a(\boldsymbol{\pi}) = &\sum_{i=1}^{M}\sum_{j=1}^{M}\sum_{k=1}^{M}\pi_{(i,j,k)}R^a_{(i,j,k)} \\ &+ \kappa\sum_{o}\left\{\max_{a'\in\mathbf{A}} U^*_{a'}\big(T_{(i,j,k)}(\boldsymbol{\pi}, a, o)\big) \times \Pr\{o \mid \boldsymbol{\pi}, a\}\right\}, \end{aligned} \tag{2.18}$$

where

$$\Pr\{o \mid \boldsymbol{\pi}, a\} = \sum_{i=1}^{M}\sum_{j=1}^{M}\sum_{k=1}^{M}\big(q^a_{(i,j,k),o}\sum_{l=1}^{M}\sum_{m=1}^{M}\sum_{n=1}^{M} p_{(l,m,n)(i,j,k)}\pi_{(l,m,n)}\big) \tag{2.19}$$

and $\mathbf{A}$ is a set of all actions. Note that the first and second terms on the right-hand side of the Equation (2.18) represent the reward obtained immediately at the decision epoch and the rewards expected to be obtained in the future, respectively. Then, the optimal policy can be derived as

$$\delta^*(\boldsymbol{\pi}) = \operatorname*{argmax}_{a\in\mathbf{A}} U^*_a(\boldsymbol{\pi}). \tag{2.20}$$

We can calculate the optimal policy by the value iteration method. The source needs to calculate the optimal policy δ^* prior to initiating its transmission. However, finding the optimal policy for a POMDP can be computationally intensive. Thus, we also seek the *myopic* policy $\hat{\delta}^*$ that maximizes the expected instantaneous reward, ignoring the impact of the current action on the future reward as follows:

$$\hat{\delta}^*(\boldsymbol{\pi}) = \underset{a \in \mathbf{A}}{\operatorname{argmax}} \sum_{i=1}^{M} \sum_{j=1}^{M} \sum_{k=1}^{M} \pi_{(i,j,k)} R^a_{(i,j,k)}. \tag{2.21}$$

A simple calculation shows that the complexity of the myopic policy is $\mathcal{O}(KM^3)$. If we consider a horizon length of τ, the complexity of the optimal policy is calculated as $\mathcal{O}(2^\tau K^\tau \beta^{\tau-1} M^6)$, where β represents the number of possible observations. The number of possible observations depends on the feedback scheme (e.g., $\beta = 2$ for ACK/NACK only scheme and $\beta = 2M$ for one-CSI feedback scheme). Therefore, finding a myopic policy instead of an optimal policy leads to a significant reduction in the complexity.

Chapter 3. Resource Management Scheme for D2D Communication in Cellular Networks

In this chapter, we propose a semi-distributed resource management framework for the D2D communication in OFDMA-based cellular networks, which aims at a high network throughput and a low signaling/computational overhead. In the proposed scheme, a two-stage resource management strategy is adopted. In the first stage, the BS allocates RBs to B2D and D2D links, based on the limited channel information which is not an accurate channel gain but the path loss of all relevant links. In the second stage, the UEs of each D2D link decide the MCS level and the transmission power for the link, while the BS schedules the transmission to/from each cellular UE on the corresponding B2D link. We consider two policies on the spatial reuse of RBs. With the first policy, multiple D2D links can coexist on the same RB, but they are not allowed to share an RB with any B2D link. The second policy is that a B2D link and multiple D2D links can be scheduled together in the same RBs.

3.1 System Model

3.1.1 Network Model

For the convenient description, we consider only an OFDMA-based cellular system, although the proposed concept can be applied to the systems using other multiple access schemes also. It is assumed that the system adopts a frequency division duplex mode. We concentrate on a single cell served by a BS as depicted in Fig. 3.1. In the cell, there are M "cellular UEs," each of which communicates *directly* with

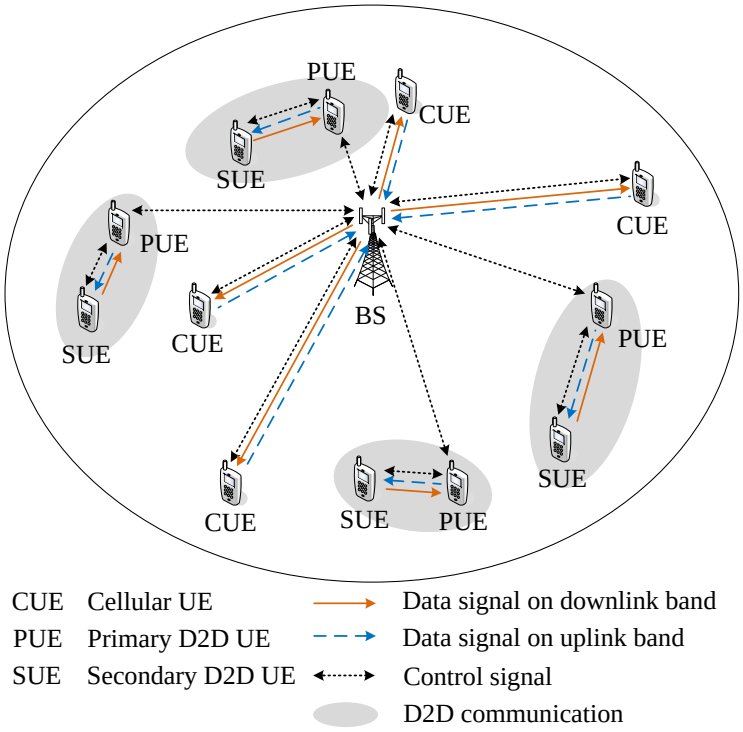

Fig. 3.1: Proposed device-to-device communication in a cellular network.

the BS. We define a "B2D link" as the bidirectional link between the BS and the corresponding cellular UE. Each B2D link is indexed by $m = 1, \ldots, M$. In the uplink (resp., downlink) band, the transmitter of B2D link m is a cellular UE (resp., the BS) and the receiver of B2D link m is the BS (resp., a cellular UE).

In addition to M cellular UEs, there are L pairs of "D2D UEs" which communicate directly with each other *without* involving the BS.[1] A "D2D link" is a peer-to-peer bidirectional link connecting two D2D UEs, one of which is called a primary D2D UE and the other is called a secondary D2D UE. We assume that a

[1] A UE can choose whether it communicates directly with another UE or involves the BS as a relay, by using a mode selection method (e.g., [49]). However, in this thesis, we will not treat a mode selection issue for concentrating on RB allocation.

D2D UE cannot dynamically alternate transmission and reception modes in each frequency band. Therefore, for enabling the communication between two D2D UEs, the primary D2D UE fixedly uses the frequency bands in a normal way (i.e., transmission in uplink band and reception in downlink band), while the secondary D2D UE uses the frequency bands the other way around (i.e., reception in uplink band and transmission in downlink band). In this setting, the primary D2D UE is capable of exchanging control signals with the BS, while the secondary D2D UE cannot. Therefore, the primary D2D UE takes charge of exchanging control signals with the BS and controlling the D2D link, and the secondary D2D UE takes orders from the primary D2D UE. The primary and secondary D2D UEs for a D2D link can be decided by considering several factors (e.g., remaining battery life, computing power). However, since the specific method is out of scope of this thesis, we will not treat this issue.

3.1.2 Radio Resource Model

A subchannel is defined as an aggregation of the fixed number of contiguous subcarriers. The uplink and downlink bands are divided into ϕ^{UL} and ϕ^{DL} subchannels, respectively. Time is divided into frames. A frame consists of τ time slots each of which occupies one or multiple OFDMA symbols. A resource block (RB) is the basic unit for radio resource allocation, consisting of one subchannel during one time slot. Hence, there are $K^{\mathrm{UL}} := \phi^{\mathrm{UL}}\tau$ uplink RBs per frame and $K^{\mathrm{DL}} := \phi^{\mathrm{DL}}\tau$ downlink RBs per frame. An RB is indexed by (b, k), where $b \in \{\mathrm{UL}, \mathrm{DL}\}$ indicates whether the RB is in the uplink band or the downlink band, and k $(= 1, \ldots, K^b)$ is the index of the RB within the corresponding band.

The BS allocates RBs to B2D and D2D links. The RBs can be categorized into

three types according to the link style: first, a "B2D-exclusive RB" is allocated to only one B2D link; second, the "D2D-exclusive RB" can be utilized for only D2D link(s), where two or more D2D links can use one D2D-exclusive RB simultaneously as long as the mutual interference is negligible; finally, in a "B2D/D2D-coexisting RB," one B2D link and one or more D2D links can be scheduled together, under the constraint that the interference between a B2D link and D2D links as well as the interference between D2D links are negligible.

3.2 Proposed Resource Management Framework

3.2.1 Framework Overview

From the temporal point of view, the proposed resource management scheme can be characterized as a two-stage scheme, where the first and second stage operations are on a long-term basis and on a short-term basis, respectively. The resource reallocation period should be short for fast adapting to the change of the time-varying communication parameters. However, the period needs to be long enough to avoid massive control messages generated from the resource allocation operation. Aiming at performance improvement, we suggest a two-stage resource management framework that compromises these conflict requirements on the reallocation period. In the (first) RB allocation stage, which is invoked with a relatively long period (e.g., several tens of frames), the BS allocates RBs to B2D links and D2D links. In the (second) transmission schedule and link control stage, of which invocation period is relatively short (typically, a frame), the BS schedules the transmission for cellular UEs by using RBs allocated to the B2D links, while the primary D2D UE of each D2D link carries out link control including the decision of MCS level

and transmission power for the link. Since the resource management functions for D2D links are distributed over BS and primary D2D UEs, the proposed scheme is a semi-distributed one from the spatial viewpoint.

3.2.2 Two-Stage Resource Management

In the proposed resource management, the RB allocator, the cellular UE scheduler, and the D2D link controller are involved. The RB allocator and the cellular UE scheduler are implemented within the BS, whereas the D2D link controller is in the primary D2D UE of each D2D link. Now, let us describe the two-stage mechanism in more detail.

First Stage (RB Allocation)

Based on the resource requests from cellular UEs and D2D UEs, the RB allocator in BS determines B2D and D2D links that can transmit simultaneously on each RB. This RB allocation is carried out periodically with a long period of time, reflecting changes in slowly varying factors such as the path loss, the average packet arrival rate, and the network topology, as follows.

At first, the D2D link controller in each primary D2D UE calculates the required numbers of RBs for uplink and downlink bands and the maximum transmission power.[2] Let N_l^{UL} and N_l^{DL} be the required numbers of RBs for D2D link l in

[2]The D2D link controller can calculate these values with various ways, considering various parameters such as the average channel quality of the link, the average traffic generation rate, the data amount in queue, and the QoS requirements. For example, assume the AMC scheme using fixed subchannel power. Let g_l and R_l be the average channel gain and the required data rate of a D2D link l, respectively. If the AMC scheme supports the data rate of $R_{\mathrm{RB}}(g_l)$ on RB under g_l, we can determine the required number of RBs in a frame for D2D link l as $N_l := \left\lceil \frac{R_l}{R_{\mathrm{RB}}(g_l)} \right\rceil$,

a frame on uplink and downlink bands, respectively. And let $P_{\mathrm{D},l}$ denote the maximum transmission power per RB for D2D link l.[3] The primary D2D UE of the D2D link l sends a "D2D resource request" containing $(N_l^{\mathrm{UL}}, N_l^{\mathrm{DL}}, P_{\mathrm{D},l})$ to the BS via the uplink control channel.

After receiving the resource requests from all primary D2D UEs, the RB allocator determines the following two sets: one is the set of B2D links that can be scheduled in RB (b,k) by the cellular UE scheduler, denoted by $\mathcal{S}_{\mathrm{C}}^{(b,k)}$; the other is the set of D2D links allowed to use RB (b,k) simultaneously, denoted by $\mathcal{S}_{\mathrm{D}}^{(b,k)}$. If RB (b,k) is a D2D-exclusive RB, we have $\mathcal{S}_{\mathrm{C}}^{(b,k)} = \emptyset$. On the other hand, if RB (b,k) is a B2D-exclusive RB, we have $\mathcal{S}_{\mathrm{D}}^{(b,k)} = \emptyset$. The RB allocator notifies the cellular UE scheduler of $\mathcal{S}_{\mathrm{C}}^{(b,k)}$ for all RBs. The RB allocator also sends the "D2D resource grant" including $\mathcal{S}_{\mathrm{D}}^{(b,k)}$ for all RBs to the primary D2D UEs, via the downlink control channel.

Second Stage (Transmission Schedule and Link Control)

The MCS level and transmission power are determined according to the link quality in this stage. The transmission on B2D links is also scheduled for the cellular UEs. These operations are conducted with a short period, in response to fast fading components and instantaneous change of data queue state.

Let us first describe the transmission *scheduling for cellular UEs* on B2D links. For each RB (b,k) such that $\mathcal{S}_{\mathrm{C}}^{(b,k)} \neq \emptyset$, the cellular UE scheduler in BS selects one B2D link out of $\mathcal{S}_{\mathrm{C}}^{(b,k)}$ and decides the transmission power and an appropriate MCS

where $\lceil x \rceil$ is the smallest integer greater than or equal to x.

[3] We assume that a D2D link uses the same maximum transmission power regardless of the RB index and the frequency band (i.e., uplink band or downlink band).

level of the B2D link on RB (b, k). We assume that the transmission power per RB of the transmitter of B2D link m is limited to $P^b_{\mathrm{C},m}$ on band b. In scheduling, the cellular UE scheduler may take account of a variety of parameters, e.g., the channel quality and the data queue state of every B2D link.

Second, let us explain the *distributed D2D link control*. The primary D2D UE for each D2D link receives the D2D resource grant, from which the primary UE finds out the set of RBs allocated to the link. For D2D link l, the set of allocated RBs is given as $\{(b, k)|l \in \mathcal{S}^{(b,k)}_{\mathrm{D}}\}$. The transmission power per RB of D2D link l is limited to the maximum transmission power $P_{\mathrm{D},l}$. The RBs allocated to a D2D link can be used for setting up not only a data channel but also a control channel of the link. The control channel is used for exchanging control information between the primary and secondary D2D UEs of the link (e.g., the reference signal, the CQI measurements, the feedbacks in hybrid automatic repeat request, etc.). The D2D link controller in each primary D2D UE independently decides the transmission power and the MCS level for each allocated RB under the condition that the transmission power is kept under the maximum transmission power $P_{\mathrm{D},l}$. For example, the D2D link controller can use a water-filling algorithm to maximize the throughput of the data channel.

3.2.3 Advantages of the Proposed Framework

The advantages of the proposed two-stage semi-distributed resource management framework are summarized as follows.

- *Distribution of Computational Burden*: The D2D link controller in each primary D2D UE independently decides the MCS level and the transmission

power for the link, which relieves the computational overhead on the BS.

- *Reduced Signaling Overhead*: The frequent CQI reports for all channels in the centralized scheme can incur a massive overhead. In the proposed framework, the RB allocator needs to know not an exact channel gain but the path loss between UEs, which can be calculated from the locations of the UEs or estimated by using the average channel qualities. In addition, since the RB (re)allocation is carried out on a long-term basis, the CQI reporting messages are not generated frequently.

- *High Network Throughput*: The typical distributed schemes exploit only the local channel information in usual. On the contrary, the proposed scheme exploits global channel information such as the path loss of all relevant links in an entire cell, which leads to a higher network throughput.

- *Easy Setting Up Control Channels for D2D Links*: A control channel between the primary and secondary D2D UEs of a D2D link can be set up on any RB(s) allocated to the D2D link in a distributed manner, which allows the spatial reuse of control channels.

- *Use of Existing Cellular UE Scheduling Algorithms*: In the proposed scheme, any existing OFDMA scheduling algorithm, which optimally allocates the transmission power and subchannels in consideration of frequency-selective fading, can be used for the cellular UE scheduler with a slight modification.

To implement the proposed resource management framework, we need the RB allocator, the cellular UE scheduler, and the D2D link controller. As mentioned above, we can use any existing OFDMA scheduling algorithm for the cellular UE

scheduler. On the other hand, since the D2D link controller in a primary D2D UE determines only the MCS level and the transmission power for the link on the granted (i.e., specified) RBs, it can be simply implemented. Thus, from now on, we concentrate on the design of an efficient RB allocator.

3.3 Conditions for Simultaneous Transmission of B2D and D2D Links

In order for an RB to be allocated to B2D and D2D links simultaneously, the mutual interference between the links should be lower than a certain threshold value. In this section, we analyze the interference on B2D and D2D links and, by using the results, derive the conditions for simultaneous allocation of an RB on B2D and D2D links. Based on the derived conditions, we will design an RB allocation algorithm in the next section.

3.3.1 Analysis of Interference on B2D and D2D Links

We use the following notations for simple description. First, let us take $g^{(b,k)}_{\mathrm{DD},i,j}$ as an example, where the symbol g represents the channel gain, the subscript "DD,i,j" means the channel from the transmitter of D2D link i to the receiver of D2D link j, and the superscript (b,k) is the RB. That is, $g^{(b,k)}_{\mathrm{DD},i,j}$ denotes the channel gain from the transmitter of D2D link i to the receiver of D2D link j on RB (b,k). In addition, let z, η, and ψ respectively represent path-loss, shadowing, multi-path fading components. Since the path-loss and shadowing components are not greatly influenced by the RB index k, we can omit the index k from the path-loss and shadowing components of a channel. Then, $z^{b}_{\mathrm{DD},i,j}$, $\eta^{b}_{\mathrm{DD},i,j}$, and $\psi^{(b,k)}_{\mathrm{DD},i,j}$

respectively denote the path-loss, shadowing, and multi-path fading components from the transmitter of D2D link i to the receiver of D2D link j on RB (b, k). Similarly, we use the subscripts "DC,i, j" and "CD,i, j" to signify the channel from the transmitter of D2D link i to the receiver of B2D link j and the channel from the transmitter of B2D link i to the receiver of D2D link j, respectively. Then, $g^{(b,k)}_{\mathrm{DD},i,j} = z^b_{\mathrm{DD},i,j}\eta^b_{\mathrm{DD},i,j}\psi^{(b,k)}_{\mathrm{DD},i,j}$, $g^{(b,k)}_{\mathrm{DC},i,j} = z^b_{\mathrm{DC},i,j}\eta^b_{\mathrm{DC},i,j}\psi^{(b,k)}_{\mathrm{DC},i,j}$, and $g^{(b,k)}_{\mathrm{CD},i,j} = z^b_{\mathrm{CD},i,j}\eta^b_{\mathrm{CD},i,j}\psi^{(b,k)}_{\mathrm{CD},i,j}$.

Let us examine the distributions of the channel gains $g^{(b,k)}_{\mathrm{DD},i,j}$, $g^{(b,k)}_{\mathrm{DC},i,j}$, and $g^{(b,k)}_{\mathrm{CD},i,j}$. The path-loss component $z^b_{\mathrm{v},i,j}$ for $\mathrm{v} \in \{\mathrm{DD}, \mathrm{DC}, \mathrm{CD}\}$ is assumed to be fixed during the time of interest. In addition, we assume that the BS knows the path-loss components between any two UEs and between any UE and the BS, based on the locations of the UEs or the average channel qualities. Furthermore, it is assumed that the shadowing components of all links over all RBs are independently and identically distributed, and the shadowing component $\eta^b_{\mathrm{v},i,j}$ follows a log-normal distribution with the mean of zero and the standard deviation of σ_η. We also assume that the multi-path components of all links over all RBs are independent of each other and all of them are exponentially distributed with the same mean of μ_ψ. According to [50], the distribution of the composite shadowing and multi-path fading can be approximated by another log-normal distribution when the shadowing component is dominant. More specifically, $g^{(b,k)}_{\mathrm{v},i,j}$ in dB (i.e., $10\log_{10} g^{(b,k)}_{\mathrm{v},i,j}$) follows the normal distribution with the mean of $10\log_{10} z^b_{\mathrm{v},i,j} + 10\log_{10}\mu_\psi - 2.5$ and the standard deviation of $\sqrt{\sigma_\eta^2 + 5.57^2}$.

Next, let us calculate the interference due to the simultaneous transmission on an RB. We define a "spatial reuse pattern" as a set of D2D links that are allocated to the same RB. Assume that the RB (b, k) is simultaneously allocated

to the B2D link m and the D2D links belonging to spatial reuse pattern $\mathcal{U}$. Since the cellular UE scheduler and each D2D link controller independently determine their own transmission power, it is reasonable that the RB allocator estimates the interference at each receiver of these simultaneous transmission links on RB (b, k) while assuming that each transmitter uses the maximum power. Recall that the transmission power per RB of D2D link l is limited to $P_{\mathrm{D},l}$ and the maximum transmission power per RB of B2D link m on band b is $P^{b}_{\mathrm{C},m}$. Then, the interference at the receiver of D2D link $l(\in \mathcal{U})$ on RB (b, k) is

$$I^{(b,k)}_{\mathrm{D},l}(\mathcal{U}, m) = \sum_{i \in \mathcal{U}, i \neq l} g^{(b,k)}_{\mathrm{DD},i,l} P_{\mathrm{D},i} + g^{(b,k)}_{\mathrm{CD},m,l} P^{b}_{\mathrm{C},m}, \tag{3.1}$$

and the interference at the receiver of B2D link m on RB (b, k) is

$$I^{(b,k)}_{\mathrm{C},m}(\mathcal{U}) = \sum_{i \in \mathcal{U}} g^{(b,k)}_{\mathrm{DC},i,m} P_{\mathrm{D},i}. \tag{3.2}$$

Next, we examine a D2D-exclusive RB (b, k) such that $\mathcal{S}^{(b,k)}_{\mathrm{D}} = \mathcal{U}$. It is noted that no B2D link is scheduled on a D2D-exclusive RB. For the convenience of description, zero value for the index of B2D link $(m = 0)$ means that no B2D link is scheduled on an RB. When $I^{(b,k)}_{\mathrm{D},l}(\mathcal{U}, 0)$ denotes the interference at the receiver of D2D link $l(\in \mathcal{U})$ on the D2D-exclusive RB (b, k),

$$I^{(b,k)}_{\mathrm{D},l}(\mathcal{U}, 0) = \sum_{i \in \mathcal{U}, i \neq l} g^{(b,k)}_{\mathrm{DD},i,l} P_{\mathrm{D},i}. \tag{3.3}$$

The interferences $I^{(b,k)}_{\mathrm{D},l}(\mathcal{U}, m)$ and $I^{(b,k)}_{\mathrm{C},m}(\mathcal{U})$ are a sum of log-normal variables, which can be approximated by another log-normal variable in the right tail [50]. Then, $I^{(b,k)}_{\mathrm{D},l}(\mathcal{U}, m)$ in dB approximately follows the normal distribution with the

mean of $\mu^b_{\mathrm{D},l}(\mathcal{U},m)$ and the standard deviation of $\sigma^b_{\mathrm{D},l}(\mathcal{U},m)$ such that

$$\sigma^b_{\mathrm{D},l}(\mathcal{U},m) = \sqrt{10\log_{10}\left(\alpha_1 \frac{\sum_{i\in\mathcal{U},i\neq l}(\zeta^b_{\mathrm{DD},i,l})^2 + (\zeta^b_{\mathrm{CD},m,l})^2}{(\sum_{i\in\mathcal{U},i\neq l}\zeta^b_{\mathrm{DD},i,l} + \zeta^b_{\mathrm{CD},m,l})^2} + 1\right)}, \tag{3.4}$$

$$\mu^b_{\mathrm{D},l}(\mathcal{U},m) = 10\log_{10}\left(\sum_{i\in\mathcal{U},i\neq l}\zeta^b_{\mathrm{DD},i,l} + \zeta^b_{\mathrm{CD},m,l}\right) + \alpha_2 - \frac{(\sigma^b_{\mathrm{D},l}(\mathcal{U},m))^2}{2}, \tag{3.5}$$

where $\alpha_1 = 10^{\frac{\sigma_\eta^2+5.57^2}{10}} - 1$, $\alpha_2 = (\sigma_\eta^2 + 5.57^2)/2$, $\zeta^b_{\mathrm{DD},i,l} := z^b_{\mathrm{DD},i,l}\mu_\psi 10^{-0.25}P_{\mathrm{D},i}$, and $\zeta^b_{\mathrm{CD},m,l} := z^b_{\mathrm{CD},m,l}\mu_\psi 10^{-0.25}P^b_{\mathrm{C},m}$.

Similarly, $I^{(b,k)}_{\mathrm{C},m}(\mathcal{U})$ in dB approximately follows the normal distribution with the mean of $\mu^b_{\mathrm{C},m}(\mathcal{U})$ and the standard deviation of $\sigma^b_{\mathrm{C},m}(\mathcal{U})$ such that

$$\sigma^b_{\mathrm{C},m}(\mathcal{U}) = \sqrt{10\log_{10}\left(\alpha_1 \frac{\sum_{i\in\mathcal{U}}(\zeta^b_{\mathrm{DC},i,m})^2}{(\sum_{i\in\mathcal{U}}\zeta^b_{\mathrm{DC},i,m})^2} + 1\right)}, \tag{3.6}$$

$$\mu^b_{\mathrm{C},m}(\mathcal{U}) = 10\log_{10}\left(\sum_{i\in\mathcal{U}}\zeta^b_{\mathrm{DC},i,m}\right) + \alpha_2 - \frac{(\sigma^b_{\mathrm{C},m}(\mathcal{U}))^2}{2}, \tag{3.7}$$

where $\zeta^b_{\mathrm{DC},i,m} := z^b_{\mathrm{DC},i,m}\mu_\psi 10^{-0.25}P_{\mathrm{D},i}$.

3.3.2 Conditions for Simultaneous Transmission of B2D and D2D Links

A *feasible* spatial reuse pattern is defined as a set of D2D links that can be scheduled together in an RB, in consideration of the interference under the condition that no B2D link is scheduled. A spatial reuse pattern $\mathcal{U}$ is feasible on RB (b,k) if and only if the following condition is met:

$$\Pr[I^{(b,k)}_{\mathrm{D},l}(\mathcal{U},0) \geq \delta] \leq \theta \qquad \forall\, l \in \mathcal{U}. \tag{3.8}$$

The probability that $I_{\mathrm{D},l}^{(b,k)}(\mathcal{U},0)$ exceeds the threshold δ is

$$\begin{aligned}\Pr[I_{\mathrm{D},l}^{(b,k)}(\mathcal{U},0) \geq \delta] &= \Pr[10\log_{10} I_{\mathrm{D},l}^{(b,k)}(\mathcal{U},0) \geq 10\log_{10}\delta] \\ &= Q\left(\frac{10\log_{10}\delta - \mu_{\mathrm{D},l}^{b}(\mathcal{U},0)}{\sigma_{\mathrm{D},l}^{b}(\mathcal{U},0)}\right),\end{aligned} \tag{3.9}$$

where $Q(\cdot)$ denotes the Q-function. Then, (3.8) can be rewritten as

$$\sigma_{\mathrm{D},l}^{b}(\mathcal{U},0)Q^{-1}(\theta) + \mu_{\mathrm{D},l}^{b}(\mathcal{U},0) \leq 10\log_{10}\delta. \tag{3.10}$$

Finally, the set of all feasible spatial reuse patterns on RB (b,k) is defined as

$$\begin{aligned}\mathcal{F}^{(b,k)} &= \{\, \mathcal{U} \mid \Pr[I_{\mathrm{D},l}^{(b,k)}(\mathcal{U},0) \geq \delta] \leq \theta \quad \forall l \in \mathcal{U}\} \\ &= \{\, \mathcal{U} \mid \sigma_{\mathrm{D},l}^{b}(\mathcal{U},0)Q^{-1}(\theta) + \mu_{\mathrm{D},l}^{b}(\mathcal{U},0) \leq 10\log_{10}\delta \quad \forall l \in \mathcal{U}\}.\end{aligned} \tag{3.11}$$

As seen from (3.11), since $\mathcal{F}^{(b,k)}$ is irrespective of k, we define $\mathcal{F}^{b}$ as a set of all feasible spatial reuse patterns for band b.

Now, we consider a B2D/D2D-coexisting RB on which a B2D link can be scheduled together with a set of D2D links. Suppose that $\mathcal{U}$ is a feasible spatial reuse pattern, i.e., $\mathcal{U} \in \mathcal{F}^{b}$. The B2D link m can be scheduled with the D2D links in $\mathcal{U}$ on RB (b,k), if the following conditions for limiting the interference by simultaneous transmission are satisfied:

$$\Pr[I_{\mathrm{C},m}^{(b,k)}(\mathcal{U}) \geq \delta] \leq \theta, \tag{3.12}$$

$$\Pr[I_{\mathrm{D},l}^{(b,k)}(\mathcal{U},m) \geq \delta] \leq \theta, \quad \forall\, l \in \mathcal{U}. \tag{3.13}$$

Similarly to (3.10), the conditions (3.12) and (3.13) can be converted to

$$\sigma_{\mathrm{C},m}^{b}(\mathcal{U})Q^{-1}(\theta) + \mu_{\mathrm{C},m}^{b}(\mathcal{U}) \leq 10\log_{10}\delta, \tag{3.14}$$

$$\sigma_{\mathrm{D},l}^{b}(\mathcal{U},m)Q^{-1}(\theta) + \mu_{\mathrm{D},l}^{b}(\mathcal{U},m) \leq 10\log_{10}\delta \quad \forall\, l \in \mathcal{U}. \tag{3.15}$$

Given a feasible spatial reuse pattern $\mathcal{U}$, we define $\Omega^b(\mathcal{U})$ as the set of all B2D links that can be scheduled together with the D2D links in $\mathcal{U}$ for band b. Then,

$$\begin{aligned}\Omega^b(\mathcal{U}) = \{\ m \mid\ & \sigma^b_{\mathrm{C},m}(\mathcal{U})Q^{-1}(\theta) + \mu^b_{\mathrm{C},m}(\mathcal{U}) \le 10\log_{10}\delta \\ & \text{and } \sigma^b_{\mathrm{D},l}(\mathcal{U},m)Q^{-1}(\theta) + \mu^b_{\mathrm{D},l}(\mathcal{U},m) \le 10\log_{10}\delta \quad \forall l \in \mathcal{U}\}.\end{aligned} \tag{3.16}$$

Recall that $\mathcal{S}_{\mathrm{D}}^{(b,k)}$ is the set of D2D links allowed to use RB (b,k) simultaneously and $\mathcal{S}_{\mathrm{C}}^{(b,k)}$ is the set of B2D links that can be scheduled in RB (b,k) by the cellular UE scheduler. In deciding $\mathcal{S}_{\mathrm{D}}^{(b,k)}$ and $\mathcal{S}_{\mathrm{C}}^{(b,k)}$, the RB allocator should check the following conditions for each type of RB.

- B2D-exclusive RB: $\mathcal{S}_{\mathrm{D}}^{(b,k)} = \emptyset$ and $\mathcal{S}_{\mathrm{C}}^{(b,k)} = \{1,\ldots,M\}$.
- D2D-exclusive RB: $\mathcal{S}_{\mathrm{D}}^{(b,k)} \in \mathcal{F}^b$ and $\mathcal{S}_{\mathrm{C}}^{(b,k)} = \emptyset$.
- B2D/D2D-coexisting RB: $\mathcal{S}_{\mathrm{D}}^{(b,k)} \in \mathcal{F}^b$ and $\mathcal{S}_{\mathrm{C}}^{(b,k)} = \Omega^b(\mathcal{S}_{\mathrm{D}}^{(b,k)})$.

3.4 Resource Block Allocation

Since the transmission power of B2D link is typically much higher than that of D2D link, when D2D links are scheduled together with a B2D link on the same RB, the D2D links may suffer severe interference from transmission of B2D link. To properly guarantee the transmission quality of D2D links, the RB allocator in BS can take the conservative reuse policy, under which D2D links cannot share the same RB with a B2D link. On the other hand, to utilize more efficiently the radio resource, the RB allocator can pursue more aggressively the spatial resource reuse, by allowing the reuse of an RB among a B2D link and D2D links as well as just among D2D links. In this section, we investigate the RB allocation problem with two policies: one is to allow the RB reuse only among D2D links, which is called

the "conservative reuse policy"; the other is named the "aggressive reuse policy," under which an RB can be allocated simultaneously to a B2D link and multiple D2D links. By solving the RB allocation problem, we can determine the number of RBs allocated to each feasible spatial reuse pattern. Given the results, any allocation is possible since the set of all feasible spatial reuse patterns is independent of the RB index k.

3.4.1 Resource Block Allocation with Conservative Reuse Policy

Problem Formulation

We formulate the RB allocation problem under the conservative reuse policy, where all RBs should be either a D2D-exclusive RB or a B2D-exclusive RB.

Since the RB allocator can solve the RB allocation problem separately for each of uplink and downlink bands using the same method, we will omit the band index b from all notations in this section. Recall that N_l denotes the required number of RBs for D2D link l in a frame. In allocating RBs, the RB allocator tries to provide at least the required number of RBs for all D2D links. We assume that there are enough RBs to satisfy the resource requests for all D2D links.[4]

In the conservative RB allocation, the goal of the RB allocator is to maximize the number of B2D-exclusive RBs, while allocating the required number of RBs to each D2D link. The RB allocator determines a set of D2D links allowed to use RB k, denoted by $\mathcal{S}_{\mathrm{D}}^{(k)}$, for all k by solving the following problem:

[4] Although this can be achieved by admission control, we will not treat the admission control for focusing on resource allocation.

$$\text{maximize} \quad \sum_{k=1}^{K} \rho_{\{\mathcal{S}_{\mathrm{D}}^{(k)}=\emptyset\}} \tag{3.17}$$

$$\text{subject to} \quad \sum_{k=1}^{K} \rho_{\{l\in\mathcal{S}_{\mathrm{D}}^{(k)}\}} \geq N_l \quad \text{for } l = 1, \ldots, L, \tag{3.18}$$

$$\mathcal{S}_{\mathrm{D}}^{(k)} \in \mathcal{F} \quad \text{for } k = 1, \ldots, K, \tag{3.19}$$

where $\rho_{\{X\}}$ is an indicator function which has 1 if X is true, and 0 otherwise. Since RB k is a B2D-exclusive RB if and only if $\mathcal{S}_{\mathrm{D}}^{(k)} = \emptyset$, the objective function in (3.17) is the number of the B2D-exclusive RBs within a frame. From the first constraint (3.18), the required number of RBs for each D2D link is guaranteed, since $\sum_{k=1}^{K} \rho_{\{l\in\mathcal{S}_{\mathrm{D}}^{(k)}\}}$ is the number of RBs allocated to D2D link l. The second constraint (3.19) means that a set of D2D links allowed to use RB k should be a feasible spatial reuse pattern.

Set Covering Problem Formulation

We rewrite the above optimization problem in the form of an integer programming problem. Suppose that there are J feasible spatial reuse patterns for a D2D-exclusive RB, i.e., $\mathcal{F} = \{\mathcal{U}_1, \ldots, \mathcal{U}_J\}$. From the set $\mathcal{F}$, we define an L-by-J matrix $\mathbf{H}$, of which the (l, j)th element is $h_{l,j} = 1$ if $l \in \mathcal{U}_j$; and $h_{l,j} = 0$ otherwise. Let a non-negative integer x_j denote the number of RBs to which $\mathcal{U}_j$ is scheduled.

Since maximizing the number of B2D-exclusive RBs means minimizing the number of D2D-exclusive RBs, the problem (3.17) – (3.19) is equivalent to

$$\text{minimize} \quad \mathbf{1}^T\mathbf{x} \tag{3.20}$$

$$\text{subject to} \quad \mathbf{H}\mathbf{x} \succeq \mathbf{N}, \tag{3.21}$$

Algorithm 1 Greedy algorithm for the set covering problem

$x_j \leftarrow 0$ for $j = 1, \ldots, J$

$\widehat{N}_l \leftarrow N_l$ for $l = 1, \ldots, L$

$\mathcal{X} \leftarrow \{1, \ldots, L\}$

while $\mathcal{X} \neq \emptyset$ **do**

  $j^* \leftarrow \text{argmax}_{j=1,\ldots,J} |\mathcal{U}_j \cap \mathcal{X}|$

  $\Delta \leftarrow \min_{l \in \mathcal{U}_{j^*} \cap \mathcal{X}} \widehat{N}_l$

  $x_{j^*} \leftarrow x_{j^*} + \Delta$

  for all $l \in \mathcal{U}_{j^*} \cap \mathcal{X}$ **do**

    $\widehat{N}_l \leftarrow \widehat{N}_l - \Delta$

    if $\widehat{N}_l = 0$ **then**

      $\mathcal{X} \leftarrow \mathcal{X} \setminus \{l\}$

    end if

  end for

end while

return $x_1, \ldots, x_J$

where $\mathbf{x} = (x_1, \ldots, x_J)^T$, $\mathbf{N} = (N_1, \ldots, N_L)^T$, '$\succeq$' denotes a component-wise inequality, and $\mathbf{1}$ is a column vector of all ones. Then, this problem can be converted to a well-known multiple set covering problem [51]. That is, when a base set is $\{1, 2, \cdots, L\}$, the subsets for covering the elements of the base set are $\mathcal{U}_1, \mathcal{U}_2, \cdots, \mathcal{U}_J$, and x_i is the number of times that $\mathcal{U}_i$ is used for covering, the problem (3.20) – (3.21) is a multiple set covering problem since its objective is to minimize $\sum_{i=1}^{J} x_i$ so that each D2D link l (an element of the base set) is covered at least as many as its required number of times, N_l.

Algorithm 2 Approximate algorithm to calculate $\mathcal{U}$ maximizing $|\mathcal{U} \cap \mathcal{X}|$ for given $\mathcal{X}$

1: $\mathcal{U} \leftarrow \emptyset$

2: $\widehat{\mathcal{X}} \leftarrow \mathcal{X}$

3: call Algorithm 3

4: $\widehat{\mathcal{X}} \leftarrow \{1, 2, \cdots, L\} \setminus \mathcal{X}$

5: call Algorithm 3

6: **return** $\mathcal{U}$

Now, we suggest a greedy algorithm for solving the proposed multiple set covering problem. In Algorithm 1, $\mathcal{X}$ is a set of unsatisfied D2D links whose RB requirements are not satisfied yet. The algorithm repeats the work to generate a feasible spatial reuse pattern $\mathcal{U}$ with the largest number of unsatisfied links (line 5) and allocate the smallest number of RBs to $\mathcal{U}$ so that at least one of unsatisfied D2D links in $\mathcal{U}$ gets the required number of RBs (line 6).

Finding $\mathcal{U}$ which maximizes $|\mathcal{U} \cap \mathcal{X}|$ over $\mathcal{U} \in \mathcal{F}$ is a challenge, since it is not a trivial task to determine whether a set of D2D links belongs to $\mathcal{F}$ or not, i.e., to determine the D2D links for which the simultaneous transmission on the same RB can be allowed. Thus, we suggest a separate approximate algorithm to find such a feasible spatial reuse pattern when a set of unsatisfied D2D links $\mathcal{X}$ is given. Line 5 in Algorithm 1 is expanded to Algorithm 2.

Since we should find $\mathcal{U}$ sharing the largest number of links with $\mathcal{X}$, Algorithm 2 first makes a feasible spatial reuse pattern $\mathcal{U}$ from the links in $\mathcal{X}$ by calling Algorithm 3, and then enlarges $\mathcal{U}$ with the links in the complementary set of $\mathcal{X}$ that are feasible to $\mathcal{U}$, by again calling Algorithm 3 in order to further increase the

Algorithm 3 Algorithm to enlarge a feasible spatial reuse pattern $\mathcal{U}$ with the links in $\widehat{\mathcal{X}}$

1: **while** $\widehat{\mathcal{X}} \neq \emptyset$ **do**
2: $l^* \leftarrow \text{argmin}_{l \in \widehat{\mathcal{X}}} \left\{ \max_{i \in \mathcal{U} \cup \{l\}} \Phi_i(\mathcal{U} \cup \{l\}) \right\}$
3: **if** $\left(\Phi_i(\mathcal{U} \cup \{l^*\}) \leq 10 \log_{10} \delta\right) \ \forall\ i \in \mathcal{U} \cup \{l^*\}$ **then**
4: $\mathcal{U} \leftarrow \mathcal{U} \cup \{l^*\}$
5: $\widehat{\mathcal{X}} \leftarrow \widehat{\mathcal{X}} \setminus \{l^*\}$
6: **for all** $l \in \widehat{\mathcal{X}}$ **do**
7: **if** $\exists i \in \mathcal{U} \cup \{l\}$ such that $\left(\Phi_i(\mathcal{U} \cup \{l\}) > 10 \log_{10} \delta\right)$ **then**
8: $\widehat{\mathcal{X}} \leftarrow \widehat{\mathcal{X}} \setminus \{l\}$
9: **end if**
10: **end for**
11: **else**
12: **return** $\mathcal{U}$
13: **end if**
14: **end while**
15: **return** $\mathcal{U}$

spatial reuse of RBs.

Algorithm 3 enlarges a feasible spatial reuse pattern $\mathcal{U}$ by repeatedly selecting a link l^* in $\widehat{\mathcal{X}}$ that is expected to generate the least amount of the interference to the D2D links in $\mathcal{U}$ and adding the link l^* to $\mathcal{U}$ if it is feasible to $\mathcal{U}$. In Algorithm 3, $\Phi_l(\mathcal{U}) \triangleq \sigma_{\mathrm{D},l}(\mathcal{U}, 0) Q^{-1}(\theta) + \mu_{\mathrm{D},l}(\mathcal{U}, 0)$, and $\widehat{\mathcal{X}}$ denotes a set of candidate links that can be added to $\mathcal{U}$. Thus, after adding the link l^*, the infeasible links for $\mathcal{U}$, i.e., the links that cannot share RBs with links in $\mathcal{U}$, are removed from $\widehat{\mathcal{X}}$ (lines 6

– 10).

We analyze the asymptotic complexity of the above algorithms. Obviously, the complexity of Algorithm 3 is $O(L^3)$. Since Algorithm 2 just calls Algorithm 3 twice, the complexity of Algorithm 2 is equal to that of Algorithm 3, i.e., $O(L^3)$. Moreover, since Algorithm 2 is executed in a while loop of Algorithm 1, the complexity of Algorithm 1 is $O(L^4)$.

3.4.2 Resource Block Allocation with Aggressive Reuse Policy

Problem Formulation

We formulate the RB allocation problem under the aggressive policy that the reuse of an RB between a B2D link and D2D links is allowed. In this problem, the RB allocator first determines a set of D2D links allowed to use an RB k, $\mathcal{S}_{\mathrm{D}}^{(k)}$. After that, it tries to find $\mathcal{S}_{\mathrm{C}}^{(k)}$, a set of the B2D links that can be scheduled together with the D2D links in $\mathcal{S}_{\mathrm{D}}^{(k)}$ while taking account of the interference. That is, $\mathcal{S}_{\mathrm{C}}^{(k)} = \Omega(\mathcal{S}_{\mathrm{D}}^{(k)})$.

Since the cellular UE scheduler independently schedules B2D links after RB allocation, the RB allocator does not have the information about, among B2D links in $\mathcal{S}_{\mathrm{C}}^{(k)}$, which B2D link will be allocated to the RB. Therefore, for an RB k, the RB allocator assumes that the RB k is expected to be allocated to each B2D link in $\mathcal{S}_{\mathrm{C}}^{(k)}$ with equal probability $1/|\mathcal{S}_{\mathrm{C}}^{(k)}|$.

The RB allocator aims at maximizing the minimum of the expected number of RBs allocated to each B2D link while satisfying the required number of RBs allocated to each D2D link. The RB allocator determines $\mathcal{S}_{\mathrm{D}}^{(k)}$ and $\mathcal{S}_{\mathrm{C}}^{(k)}$ for all k

by solving the following problem:

$$\text{maximize} \qquad \min_{m=1,\ldots,M} \sum_{k=1}^{K} \frac{\rho_{\{m\in\mathcal{S}_{\mathrm{C}}^{(k)}\}}}{|\mathcal{S}_{\mathrm{C}}^{(k)}|} \tag{3.22}$$

$$\text{subject to} \qquad \sum_{k=1}^{K} \rho_{\{l\in\mathcal{S}_{\mathrm{D}}^{(k)}\}} \geq N_l \quad \text{for } l = 1,\ldots,L, \tag{3.23}$$

$$\mathcal{S}_{\mathrm{C}}^{(k)} = \Omega\big(\mathcal{S}_{\mathrm{D}}^{(k)}\big) \quad \text{for } k = 1,\ldots,K, \tag{3.24}$$

$$\mathcal{S}_{\mathrm{D}}^{(k)} \in \mathcal{F} \quad \text{for } k = 1,\ldots,K. \tag{3.25}$$

The objective function in (3.22) is the minimum of the expected number of RBs allocated to each B2D link. This objective is set to provide max-min fair allocation. From the constraint in (3.23), the required number of RBs for each D2D link is guaranteed.

Linear Programming Formulation

The above optimization problem can simply be converted to an integer programming (IP) problem. Recall that there are J feasible spatial reuse patterns, $\mathcal{F} = \{\mathcal{U}_1,\ldots,\mathcal{U}_J\}$, and the matrix $\mathbf{H}$ is defined such that the (l,j)th entry of $\mathbf{H}$ is $h_{l,j} = 1$ if $l \in \mathcal{U}_j$; and $h_{l,j} = 0$ otherwise. In addition, we also define an M-by-J matrix $\mathbf{Y}$. The (m,j)th entry of $\mathbf{Y}$ is $y_{m,j} = 1/\big|\Omega\big(\mathcal{U}_j\big)\big|$ if $m \in \Omega\big(\mathcal{U}_j\big)$; and $y_{m,j} = 0$ otherwise.

From $\mathbf{H}$ and $\mathbf{Y}$, the optimization problem equivalent to the problem (3.22) –

(3.25) is given as

$$\begin{aligned}
\text{maximize} \quad & \beta && (3.26)\\
\text{subject to} \quad & \mathbf{Hx} \succeq \mathbf{N}, && (3.27)\\
& \mathbf{Yx} \succeq \beta\mathbf{1}, && (3.28)\\
& \mathbf{1}^T\mathbf{x} \leq K, && (3.29)\\
& \mathbf{x} \succeq \mathbf{0}, && (3.30)\\
& \beta \geq 0, && (3.31)
\end{aligned}$$

where β is a slack variable, $\mathbf{x} = (x_1, \ldots, x_J)^T$, and $\mathbf{0}$ is a column vector of all zeros. Remind that a non-negative integer x_j in the vector $\mathbf{x}$ is the number of RBs to which $\mathcal{U}_j$ is scheduled.

If the variable x_j for all j is relaxed to be a real value, the above IP problem becomes a linear programming (LP) problem. Although an LP problem can be solved by a standard method such as the simplex method, the size of this problem is too large to be solved by such a method especially due to the exponential increase of J according to the number of D2D links. Hence, we suggest to use the column generation method to solve this problem.

Column Generation Method

In the column generation approach, the problem is decomposed into the master problem and the subproblem. First, the master problem with the matrix (e.g., corresponding to $\mathbf{H}$ and $\mathbf{Y}$ in our problem) consisting of only a few columns is solved. Based on the solution, the subproblem is solved to obtain a new column to be added to the matrix of the master problem. This procedure is repeated

iteratively until a stopping criterion is satisfied. Thus, the key idea of the column generation is to improve the solution by gradually increasing the number of the columns of the matrix at each iteration. For more details on the column generation approach, one can refer to [52].

We use Lagrange duality to efficiently search new columns at each step, like in [53]. By introducing Lagrange multipliers $\boldsymbol{\lambda} = (\lambda_1, \lambda_2, \ldots, \lambda_L)^T$, $\boldsymbol{\nu} = (\nu_1, \nu_2, \ldots, \nu_M)^T$, and ξ, the dual problem of the optimization problem (3.26) – (3.31) is derived as follows:

$$\begin{aligned}
\text{minimize} \quad & -\boldsymbol{\lambda}^T\mathbf{N} + K\xi && (3.32)\\
\text{subject to} \quad & \boldsymbol{\lambda}^T\mathbf{H} + \boldsymbol{\nu}^T\mathbf{Y} - \mathbf{1}^T\xi \preceq \mathbf{0}^T, && (3.33)\\
& 1 - \boldsymbol{\nu}^T\mathbf{1} \leq 0, && (3.34)\\
& \boldsymbol{\lambda} \succeq \mathbf{0}, && (3.35)\\
& \boldsymbol{\nu} \succeq \mathbf{0}, && (3.36)\\
& \xi \geq 0, && (3.37)
\end{aligned}$$

which we call the *master problem*.

The column generation method solves the master problem and the subproblem at each iteration. At the ith iteration, the column generation method maintains the matrices $\widetilde{\mathbf{H}}^{(i)}$ and $\widetilde{\mathbf{Y}}^{(i)}$ corresponding to $\mathbf{H}$ and $\mathbf{Y}$, respectively. The matrices $\widetilde{\mathbf{H}}^{(i)}$ and $\widetilde{\mathbf{Y}}^{(i)}$ can be viewed as a reduced version of $\mathbf{H}$ and $\mathbf{Y}$, only having some columns of $\mathbf{H}$ and $\mathbf{Y}$, respectively. Let $\mathbf{h}_j$ and $\mathbf{y}_j$ respectively denote the jth column of the matrices $\mathbf{H}$ and $\mathbf{Y}$. That is, $\mathbf{h}_j = (h_{1,j}, \ldots, h_{L,j})^T$ and $\mathbf{y}_j = (y_{1,j}, \ldots, y_{M,j})^T$. Then, each column of $\widetilde{\mathbf{H}}^{(i)}$ and $\widetilde{\mathbf{Y}}^{(i)}$ are respectively equal to $\mathbf{h}_j$ and $\mathbf{y}_j$ for some $j = 1, \ldots, J$. At the first iteration, the column generation method starts with $\widetilde{\mathbf{H}}^{(1)}$

and $\widetilde{\mathbf{Y}}^{(1)}$ which consist of easily identifiable columns in $\mathbf{H}$ and $\mathbf{Y}$.

At the ith iteration, the column generation method solves the master problem (3.32) – (3.37) with the constraint (3.33) replaced by $\boldsymbol{\lambda}^T\widetilde{\mathbf{H}}^{(i)} + \boldsymbol{\nu}^T\widetilde{\mathbf{Y}}^{(i)} - \mathbf{1}^T\xi \preceq \mathbf{0}^T$. The master problem can be solved by means of the simplex method. The solutions of the master problem at the ith iteration are denoted by $\widetilde{\boldsymbol{\lambda}}^{(i)}$, $\widetilde{\boldsymbol{\nu}}^{(i)}$, and $\widetilde{\xi}^{(i)}$.

After the solutions of the master problem are obtained, the column generation method solves the subproblem to add new columns to $\widetilde{\mathbf{H}}^{(i)}$ and $\widetilde{\mathbf{Y}}^{(i)}$. The matrices for the next iteration $\widetilde{\mathbf{H}}^{(i+1)}$ and $\widetilde{\mathbf{Y}}^{(i+1)}$ are obtained by adding new columns $\widetilde{\mathbf{h}}$ and $\widetilde{\mathbf{y}}$ such that $\widetilde{\mathbf{H}}^{(i+1)} = [\widetilde{\mathbf{H}}^{(i)}\ \widetilde{\mathbf{h}}]$ and $\widetilde{\mathbf{Y}}^{(i+1)} = [\widetilde{\mathbf{Y}}^{(i)}\ \widetilde{\mathbf{y}}]$. The new columns, which contribute most to improve the solution, can be derived by solving the following subproblem.

$$\text{maximize} \qquad \left(\widetilde{\boldsymbol{\lambda}}^{(i)}\right)^T\widetilde{\mathbf{h}} + \left(\widetilde{\boldsymbol{\nu}}^{(i)}\right)^T\widetilde{\mathbf{y}} - \widetilde{\xi}^{(i)} \tag{3.38}$$

$$\text{subject to} \qquad \widetilde{\mathbf{h}} = \mathbf{h}_j \text{ and } \widetilde{\mathbf{y}} = \mathbf{y}_j \text{ for some } j. \tag{3.39}$$

Solving this subproblem is not trivial since finding $\widetilde{\mathbf{h}}$ and $\widetilde{\mathbf{y}}$, which satisfy the constraint in (3.39), is equivalent to finding a feasible spatial reuse pattern and the corresponding set of B2D links.

In Algorithm 4, we present a greedy algorithm for solving the subproblem (3.38) – (3.39). In Algorithm 4, $\Xi(\mathcal{U})$ is defined as $\Xi(\mathcal{U}) = \sum_{l\in\mathcal{U}}\widetilde{\lambda}_l^{(i)} + \sum_{m\in\Omega(\mathcal{U})}\frac{\widetilde{\nu}_m^{(i)}}{|\Omega(\mathcal{U})|}$. Algorithm 4 adds a D2D link to $\mathcal{U}$ one by one at each stage by selecting the link l^* which most increases the value of the objective function in (3.38). After adding the link l^*, the D2D links that cannot be added to $\mathcal{U}$ are removed in advance (lines 9 – 13 in Algorithm 4).

After deriving the solution of the subproblem (i.e., $\widetilde{\mathbf{h}}$ and $\widetilde{\mathbf{y}}$), the matrices $\widetilde{\mathbf{H}}^{(i+1)}$ and $\widetilde{\mathbf{Y}}^{(i+1)}$ are generated by adding the new columns $\widetilde{\mathbf{h}}$ and $\widetilde{\mathbf{y}}$ to $\widetilde{\mathbf{H}}^{(i)}$ and $\widetilde{\mathbf{Y}}^{(i)}$,

Algorithm 4 Approximate algorithm for solving the subproblem to calculate $\widetilde{\mathbf{h}}$ and $\widetilde{\mathbf{y}}$

$\mathcal{U} \leftarrow \emptyset$

$\omega \leftarrow \sum_{m=1}^{M} \left(\widetilde{\nu}_m^{(i)}/M\right)$

$\mathcal{X} \leftarrow \{1, \ldots, L\}$

while $\mathcal{X} \neq \emptyset$ and $\omega < \max_{l \in \mathcal{X}} \Xi(\mathcal{U} \cup \{l\})$ **do**

  $l^* = \text{argmax}_{l \in \mathcal{X}} \Xi(\mathcal{U} \cup \{l\})$

  $\mathcal{U} \leftarrow \mathcal{U} \cup \{l^*\}$

  $\mathcal{X} \leftarrow \mathcal{X} \setminus \{l^*\}$

  $\omega \leftarrow \Xi(\mathcal{U})$

  for all $l \in \mathcal{X}$ **do**

    if $\exists i \in \mathcal{U} \cup \{l\}$ such that $\left(\Phi_i(\mathcal{U} \cup \{l\}) > 10 \log_{10} \delta\right)$ **then**

      $\mathcal{X} \leftarrow \mathcal{X} \setminus \{l\}$

    end if

  end for

end while

$\widetilde{h}_l \leftarrow 1$ for $l \in \mathcal{U}$

$\widetilde{h}_l \leftarrow 0$ for $l \notin \mathcal{U}$

$\widetilde{y}_m \leftarrow 1/|\Omega(\mathcal{U})|$ for $m \in \Omega(\mathcal{U})$

$\widetilde{y}_m \leftarrow 0$ for $m \notin \Omega(\mathcal{U})$

return h and y

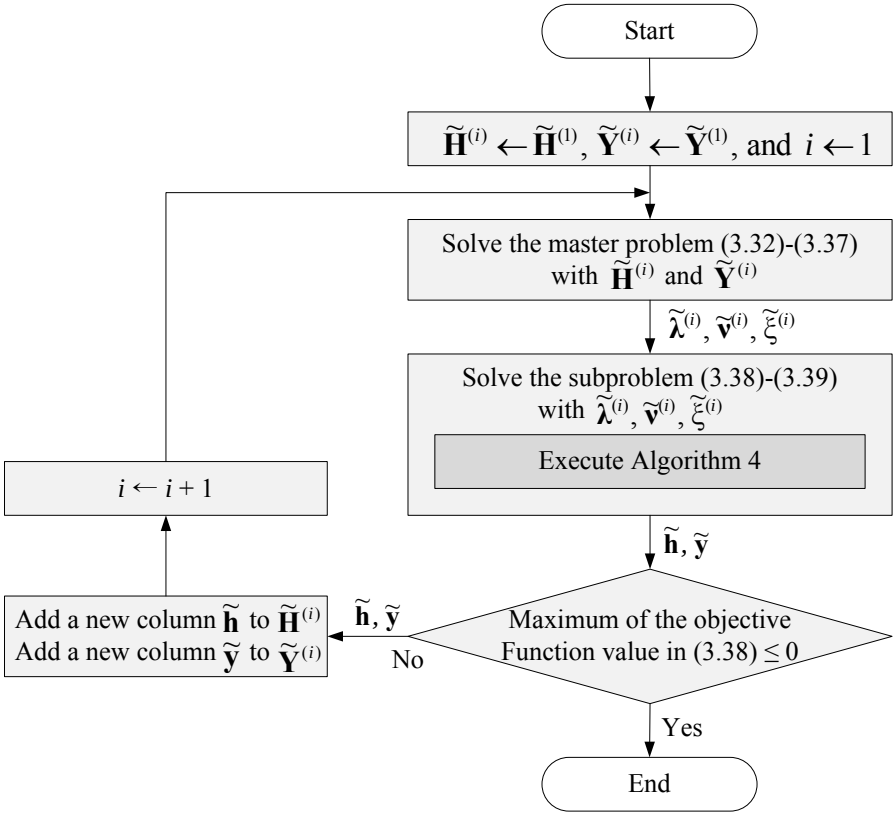

Fig. 3.2: Overall procedure for the column generation.

respectively. At the $(i+1)$th iteration, the master problem and the subproblem with the matrices $\widetilde{\mathbf{H}}^{(i+1)}$ and $\widetilde{\mathbf{Y}}^{(i+1)}$ are solved. This procedure is repeated until the solution of the master problem is not increased by adding a new column. That is, if the maximum value of the objective function (3.38) is less than or equal to zero, the column generation procedure is terminated. The overall procedure for the column generation is summarized in Fig. 3.2.

Let us analyze the asymptotic complexity of the column generation in Fig. 3.2. It is obvious that the complexity of Algorithm 4 is $O(L^3)$. The number of added columns (or iterations) in the column generation is limited to 2^L. However, since a new column which contributes most to improve the solution is added in each iteration, the column generation is terminated after much fewer iterations in practice. In other words, when κ is the average number of iterations, $\kappa \ll 2^L$. Accordingly, the complexity of the column generation is $O(L^3\kappa)$.

Chapter 4. Performance Evaluation

4.1 Adaptive Transmission Scheme for Cooperative Communication

4.1.1 Simulation Model

For the nominal values of simulation parameters, we refer to IEEE 802.11g system where the channel bandwidth is 10 MHz and the center frequency is 2.4 GHz. The relay is assumed to be located in the middle between the source and the destination. We consider 4 different MCS levels: 4-QAM, 8-QAM, 16-QAM, and 64-QAM with the same (7, 5) RS code. The length of a frame T_F is 1 ms. The sizes of an ACK packet, an ACK packet with one CSI feedback, and an ACK packet with two CSI feedback are set to 134, 137, and 140 bits, respectively. In addition, all packet transmissions are separated by a short constant time spacing of 32 μs, irrespective of packet type. With these parameters, the lengths of packet transmissions in the proposed schemes are $T_0 = 848$ μs, $T_1 = 408$ μs, and $T_{ACK} = 88$ μs [see Fig. 2.1].

We consider the path loss and the multi-path fading as the channel model. We use simplified path loss model in [47] assuming that the path loss exponent is 3.5. Rayleigh fading is generated by Jakes' model [45]. The maximum Doppler frequency f_d is set to 10 Hz which is the same fading rate as that of a pedestrian with the moving speed of 4.5 km/h. We consider the FSMC model with eight channel states (i.e., $M = 8$). The thresholds of the received SNR $\mathbf{\Gamma}$ are set to $\Gamma_i = 5 + 3.5 \times (i - 2)$ dB, for $i \in 2, 3, \ldots, M$. The transmission power ρ, noise spectral density N_0, and discount factor κ are set to 10 mW, -163 dBm/Hz, and 0.95, respectively.

4.1.2 Simulation Results

Figs. 4.1 and 4.2 show the trace of actions, estimated channel states, and observations of the ACK/NACK only and one-CSI feedback schemes. The average SNR of SD channel is set to 15 dB. For comparison, the same sequence of channel variations is used for these figures. An estimated channel state of each feedback scheme represents the state which has the highest marginal belief value in the corresponding channel (e.g., the marginal belief value of state i in SD channel is calculated as $\sum_j \sum_k \pi_{i,j,k}$). In these two schemes, the SR and RD channels can be treated from the standpoint of the source as one "SR–RD composite channel," the SNR of which is a function of the SNRs of the SR and RD channels. The SNR of the SR–RD composite channel is calculated as $\frac{\gamma^{(SR)}\gamma^{(RD)}}{\gamma^{(SR)}+\gamma^{(RD)}+1}$. Note that, when the network selects the direct transmission, the estimated state of the SR–RD composite channel does not change because it cannot acquire any information about the SR–RD composite channel state [e.g., (C) of Fig. 4.2].

From the first half of Fig. 4.1, we can see that the decision switches from the direct transmission to the cooperative transmission [see (A) in Fig. 4.1] when the SD channel is estimated to be relatively worse than the SR–RD composite channel. In contrast, when the opposite situation occurs as shown in the second half of these figures, the decision switches from the cooperative transmission to the direct transmission [see (B) in Fig. 4.1]. In the ACK/NACK only scheme, switching between the direct transmission and the cooperative transmission occurs later than that of the one-CSI feedback scheme as depicted in the regions (A) and (B) of Fig. 4.1. This means that the adaptation speed of the ACK/NACK only scheme is slower than that of the one-CSI feedback scheme, mainly due to

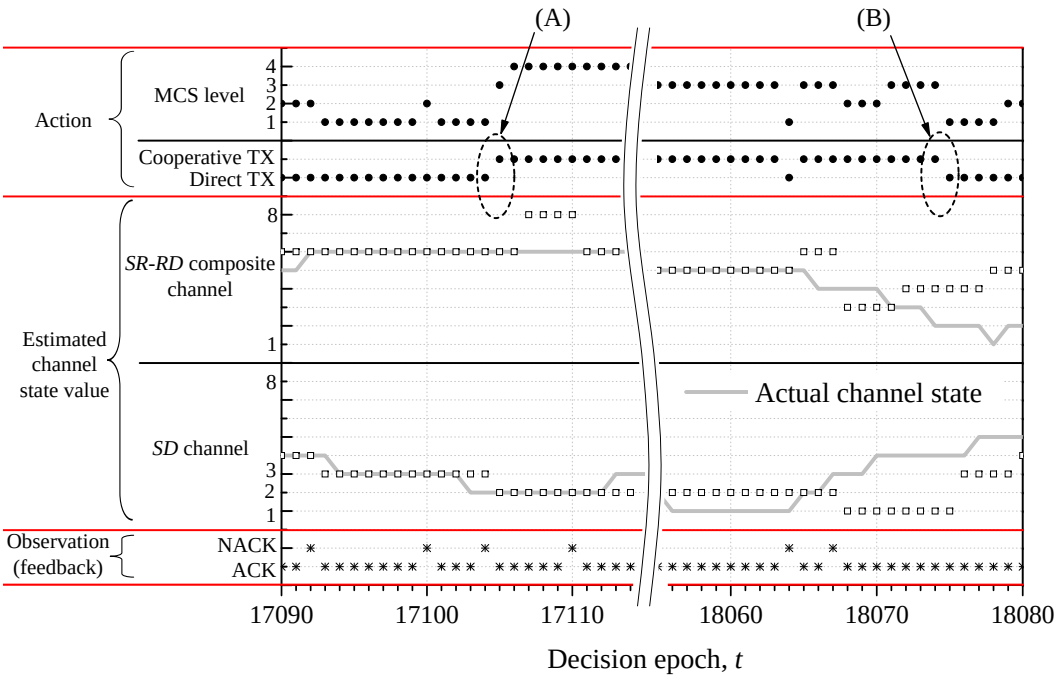

Fig. 4.1: Trace of estimated channel states, actions, and observations for ACK/NACK only scheme.

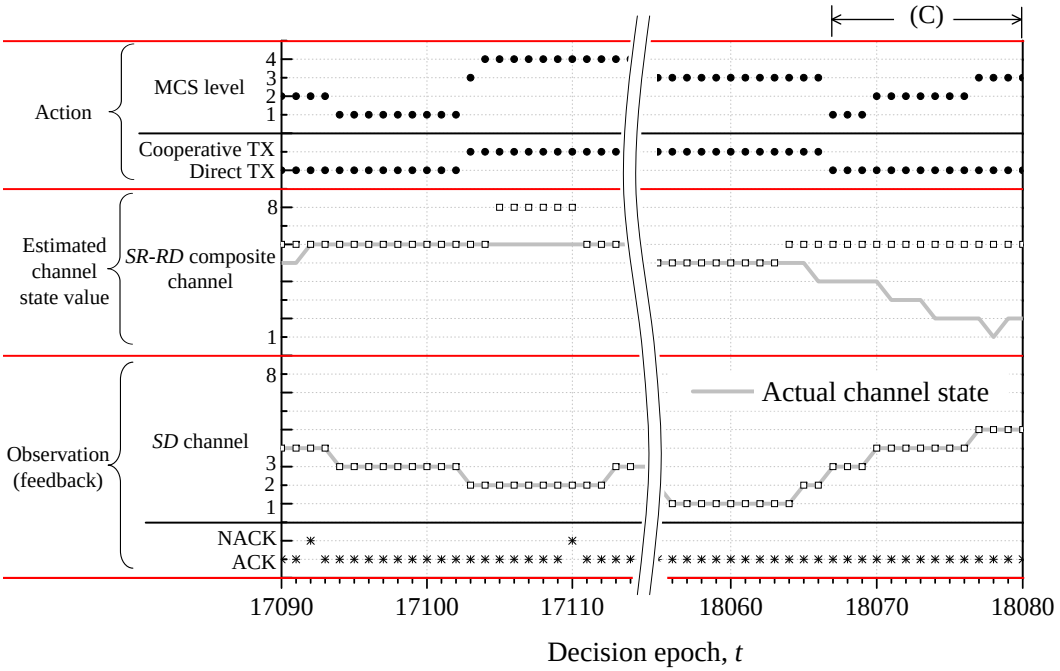

Fig. 4.2: Trace of estimated channel states, actions, and observations for one-CSI feedback scheme.

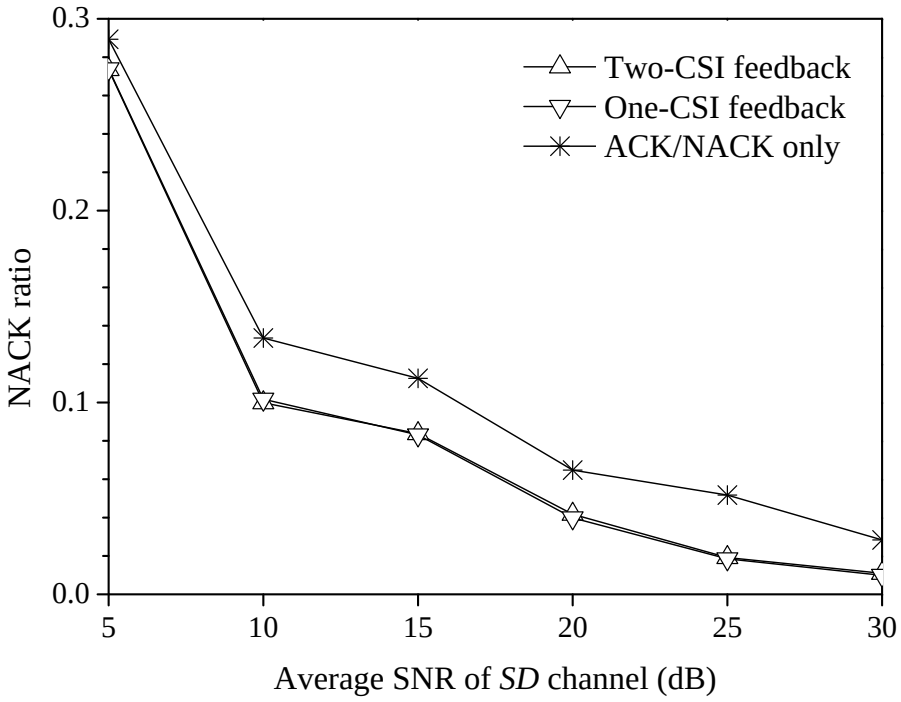

Fig. 4.3: NACK ratio comparison between the proposed feedback schemes.

the errors in estimating the SD channel state. Also, the ACK/NACK only scheme more frequently makes an inappropriate decision than the one-CSI feedback scheme, yielding a larger number of NACKs. In the case of one-CSI feedback scheme, we can see from the period (C) of Fig. 4.2 that, as the SD channel state gets better, the network adapts properly to the good channel state by increasing the MCS level.

In Figs. 4.3 and 4.4, we investigate the impact of the amount of feedback overhead on the performance of the proposed scheme. In Fig. 4.3, the "NACK ratio" is defined as the ratio of the number of frames that the NACK packet is returned to the total number of frames. This figure shows that the ACK/NACK

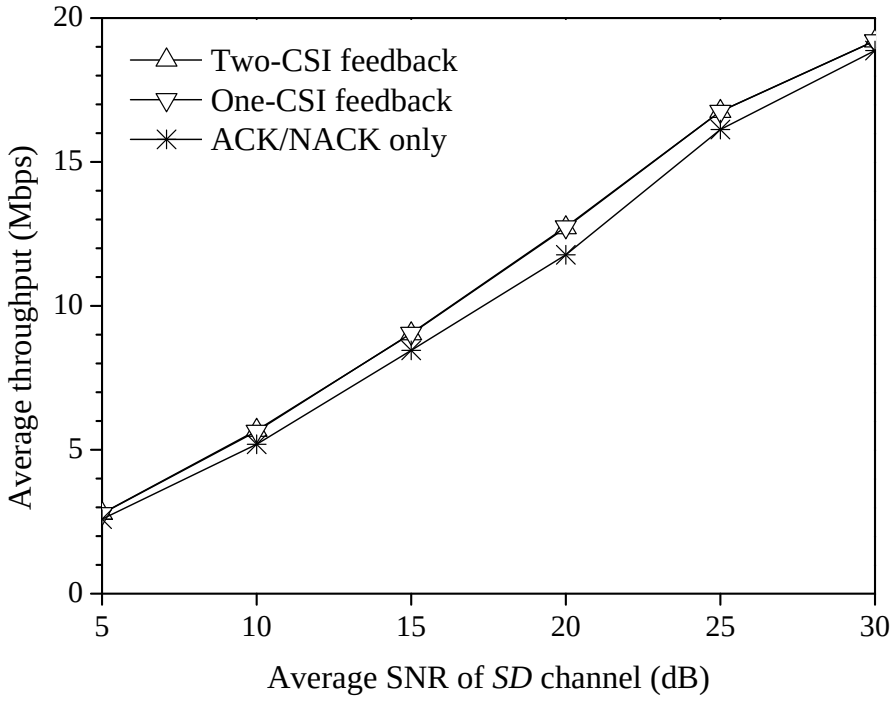

Fig. 4.4: Throughput comparison between the proposed feedback schemes.

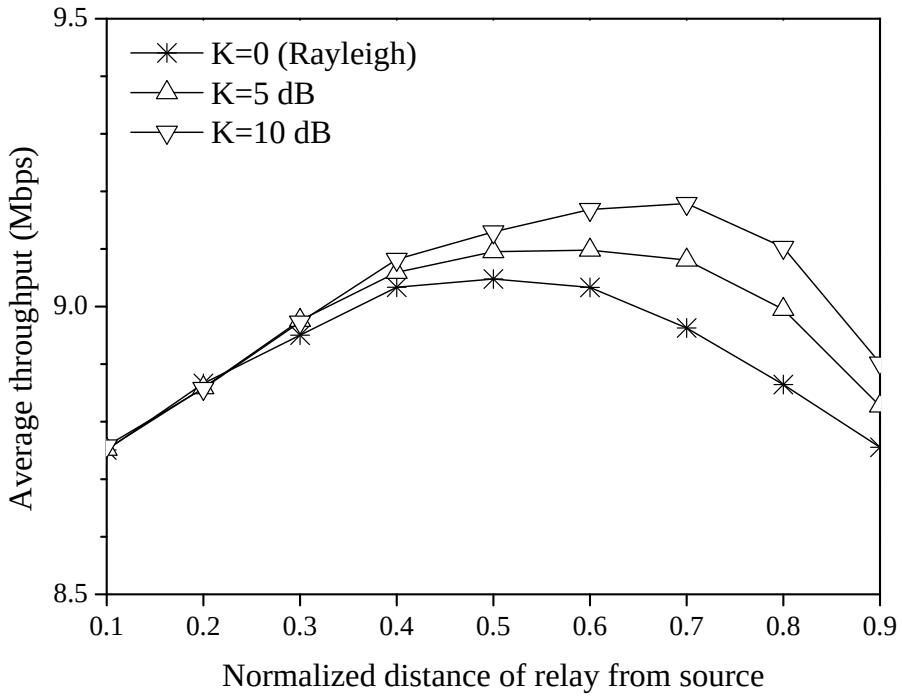

Fig. 4.5: Effect of the location of relay and Rician fading.

only scheme has a higher NACK ratio since it makes less optimal decision than the other schemes. Consequently, the ACK/NACK only scheme achieves slightly lower throughput than the one-CSI and two-CSI feedback schemes as shown in Fig. 4.4. The one-CSI feedback scheme has almost the same throughput as that of the two-CSI feedback scheme despite of less feedback information. From now on, we use the one-CSI feedback scheme as the representative scheme.

Now, we investigate in Fig. 4.5 the effect of the location of the relay and the Rician fading on the performance of the proposed one-CSI feedback scheme when the average SNR of SD channel is 15 dB. The Rician fading is assumed only on SR

channel and is generated by the model in [55]. The K-factor in the Rician fading is defined as the ratio of the power of the dominant direct path component to the power of the remaining path components. The distance of the relay from the source is normalized by the distance between the source and destination. Since a larger K-factor implies less severe fading, the average throughput increases as the K-factor increases. The optimal location of the relay, in terms of average throughput, moves toward the destination when the K-factor increases. This is because the improving the quality of the more unstable channel (i.e., RD channel) helps the estimation of the SR–RD composite channel state.

Now, we compare the performance of the proposed scheme with those of two schemes, called the "direct scheme" and the "full feedback scheme." The direct scheme is a simple baseline scheme where the source always transmits a packet directly to the destination with the MCS level chosen based on the CSI of SD channel. In the full feedback scheme, the SNRs of all channels are estimated and fed back every frame. The SNRs of the SD channel and the RD channel are piggybacked on the ACK/NACK packet, like in the proposed two-CSI feedback scheme. In addition, the SNR of the SR channel is explicitly reported from the relay to the source every frame. The time for reporting the SNR of the SR channel, T_{RP}, is assumed to be equal to the transmission time of an ACK packet. Thus, the lengths of packet transmissions in the full feedback scheme are $T_0 = 728$ μs, $T_1 = 348$ μs, and $T_{ACK} = T_{RP} = 88$ μs. In the full feedback scheme, the source selects the action a^* which maximizes the instantaneous expected throughput, i.e., $a^* = \text{argmax}_{(l,y)\in\mathbf{A}} \left\{ r_l(B_y) \times \left(1 - \psi_{\text{pkt}}(\tilde{\boldsymbol{\gamma}}, l, y)\right) \right\}$, where $\tilde{\boldsymbol{\gamma}}$ is the reported SNRs of all channels.

Fig. 4.6 compares the performance of the one-CSI feedback scheme with those

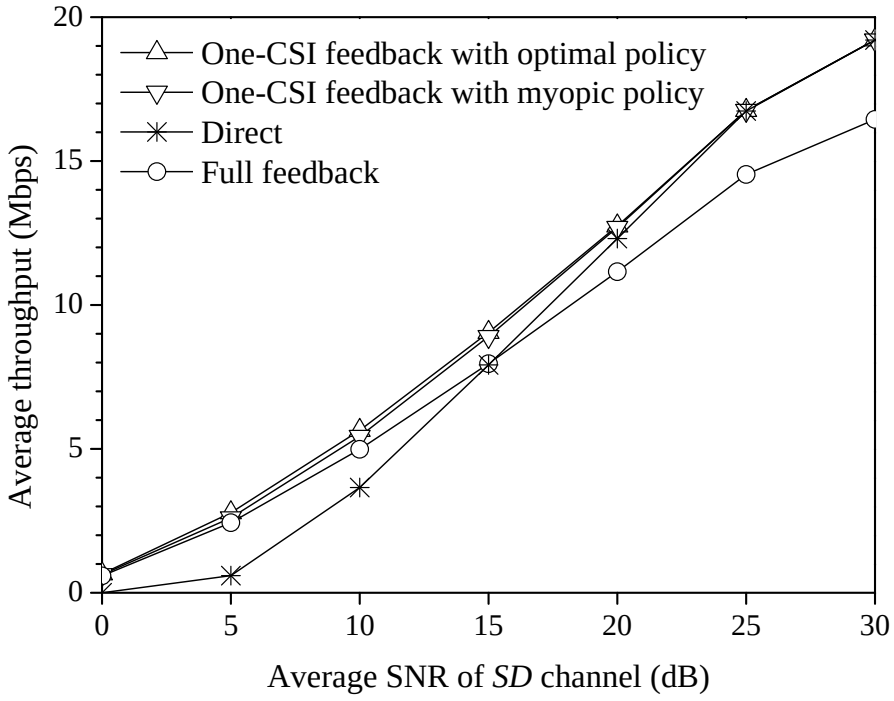

Fig. 4.6: Performance comparison between the proposed one-CSI feedback and the other three schemes.

of the full feedback and the direct schemes according to the average SNR of SD channel. When the average SNR of SD channel is high (around 20–30 dB in the figure), the full feedback scheme performs worse than the direct scheme. This is caused by high feedback overhead of the full feedback scheme. On the other hand, the proposed scheme has similar throughput to that of the direct scheme when the average SNR of SD channel is high, because of its low feedback overhead. In addition, when the average SNR of SD channel is low, the proposed scheme takes advantage of cooperative transmission via the relay, like the full feedback scheme. Consequently, the proposed scheme outperforms the full feedback scheme in all ranges of the average SNR of SD channel. We can also observe from the figure that the performance of the proposed scheme using the myopic policy is comparable to that of the proposed scheme using the optimal policy. When the average SNR of SD channel is 20 dB, 96% of the actions taken by the myopic policy are the same as those taken by the optimal policy out of 3 million epochs. Therefore, the myopic policy can be a low-complexity alternative to the optimal policy.

Table 4.1 shows the impacts that the maximum Doppler frequency has on the performance of the one-CSI feedback, full feedback, and direct schemes, when the average SNR of SD channel is 10 dB. In all of three schemes, as the maximum Doppler frequency increases, the average throughput slightly decreases due to the increase of the errors in estimating the channel state. Nevertheless, the one-CSI feedback scheme with the low-complexity myopic policy still achieves a higher throughput than the full feedback and direct schemes.

Tab. 4.1: Effect of the maximum Doppler frequency f_d on the performance of the schemes

Scheme	**Average throughput (Mbps)**		
	$f_d = 10$ Hz	$f_d = 20$ Hz	$f_d = 30$ Hz
Direct	3.66	3.62	3.60
Full feedback	4.99	4.93	4.84
One-CSI feedback with myopic policy	5.44	5.34	5.29
One-CSI feedback with optimal policy	5.62	5.46	5.37

4.2 Resource Management Scheme for D2D Communication in Cellular Networks

4.2.1 Simulation Model

For a realistic simulation, the simulation parameter values are chosen based on those in the LTE system [54]. There are 50 cellular UEs and L D2D links within a single circular cell with the radius of 300 m. We assume that a frame is composed of 10 time slots ($\tau = 10$) and there are 50 subchannels in the uplink and downlink bands, respectively ($\phi^{\mathrm{DL}} = \phi^{\mathrm{UL}} = 50$). Thus, the total number of RBs in a frame is 500 for each of uplink and downlink bands ($K^{\mathrm{UL}} = K^{\mathrm{DL}} = 500$). Each subchannel consists of 12 subcarriers. Also, it is assumed that the bandwidth of an RB is $W_{\mathrm{RB}} = 180$ kHz and the noise spectral density is $N_0 = -174$ dBm/Hz. The simulator is developed using Matlab software. Specifically, LP problems in the proposed schemes are solved with the interior-point method by using *linprog*

function in Matlab.

The path-loss, shadowing, and Rayleigh fading are considered. The path-loss model is that $z = 35.3 + 37.6 \log_{10} d$ (dB) where d is the distance between the transmitter and receiver. The parameter values for shadowing and Rayleigh fading are $\sigma_\eta = 8$ dB and $\mu_\psi = 1$, and the threshold values for simultaneous transmission condition are $\delta = -107$ dBm and $\theta = 0.01$.

The interval of RB allocation is set to 100 frames and the simulation run time is 500 intervals. During the simulation, at the start of each RB allocation interval, the cellular UEs are randomly located within a cell and L D2D links are also randomly positioned in a cell with the constraint that the distance between the primary and secondary D2D UEs is less than 10 m. At the start of RB allocation interval, for each D2D link l, a transmission power per RB, P_l, is calculated such that the average received signal-to-noise ratio (SNR), $\frac{z_l P_l}{W_{\mathrm{RB}} N_0}$, is 9 dB. The UEs of D2D link l transmit with this fixed power P_l during the corresponding interval. The transmission powers of the BS and a cellular UE on a B2D-exclusive RB are fixed as 400 mW and 5 mW, respectively. For a B2D/D2D-coexisting RB, the BS and a cellular UE transmit using their respective fixed powers calculated such that the average SNR at the receiver is 5.6 dB on uplink and 9 dB on downlink, during the corresponding RB allocation interval.

At the start of each RB allocation interval, the RB allocator determines S_{D} and S_{C} for each RB in a frame on uplink and downlink, using the proposed schemes of Section V. In the simulation, $N_l^{\mathrm{UL}} = N_l^{\mathrm{DL}} = 25$ RBs for all D2D links. With the RB allocation results, every frame the cellular UE scheduler performs the round-robin scheduling on B2D-exclusive RBs and the Max C/I scheduling on B2D/D2D-coexisting RBs. The data rate of a transmitter on its allocated RB is

adaptively controlled according to channel quality every frame. Since we assume the continuous-rate M-ary quadrature amplitude modulation for link adaptation, the data rate of a link l for RB (b,k) is $W_{\mathrm{RB}} \log_2(1 + \frac{-1.5}{ln(5\times BER)}\gamma_l^{(b,k)})$ bps [56], where $\gamma_l^{(b,k)}$ is the received SINR at the receiver of the link l on the RB (b,k) and BER is the target bit error rate which we set to 0.01.

4.2.2 Simulation Results

We examine the performance characteristics of the proposed RB allocation schemes in Figs. 4.7 – 4.11. First, let us investigate the optimality gaps of the proposed schemes, by taking the value of the objective function as a measure. Since the results on DL band show the similar tendency with those on UL band, we present only the results on UL band in Figs. 4.7 and 4.8. Fig. 4.7 shows a heuristic solution from the proposed greedy algorithm (Algorithms 1 – 3) and the optimal solution, for the conservative RB allocation problem. The optimal solution of the problem is obtained by solving the LP problem (3.20) – (3.21) with all columns of the $\mathbf{H}$, which are generated by the exhaustive search. We can observe from the figure that the constraint is well satisfied with the proposed greedy algorithm, and furthermore the heuristic solution is almost the same as the optimal solution in the number of B2D-exclusive RBs within a frame. This means that the proposed greedy algorithm finds the D2D links very efficiently with low computational complexity. On the other hand, Fig. 4.8 shows the results for the aggressive RB allocation, where the "optimal" values are obtained by solving the primal problem (3.26) – (3.31) with all columns of the $\mathbf{H}$ and $\mathbf{Y}$ at the first iteration. As seen from Fig. 4.8, the value of objective function is almost the same as its optimal value. In other words, the aggressive scheme can achieve the near-optimal performance while guaranteeing

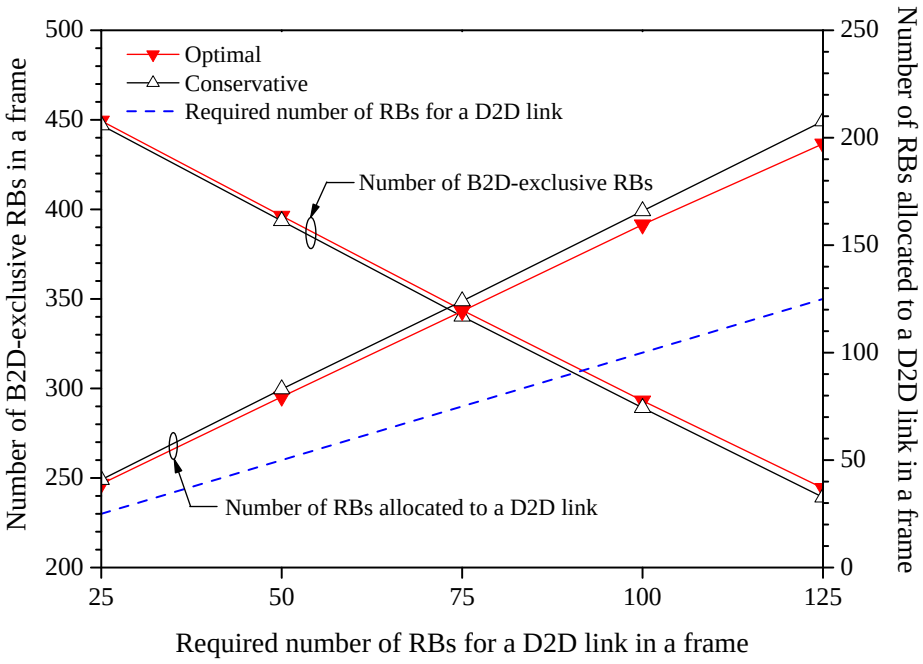

Fig. 4.7: Optimality gap of the conservative scheme when there are ten D2D links in a cell.

the resource requirements of D2D links.

Next, we evaluate the spatial reuse performance of the proposed schemes in Figs. 4.9 and 4.10, where only the results on UL band are presented because the results on DL band are almost the same as those on UL band. As observed from Fig. 4.9, in both of the conservative and aggressive schemes, the average number of D2D links allocated simultaneously on the same RB increases as the number of D2D links in a cell increases. However, when there are more D2D links in a cell, the percentage of D2D links allocated on the same RB among the whole of D2D links is reduced because the shorter distance between D2D links may incur the higher

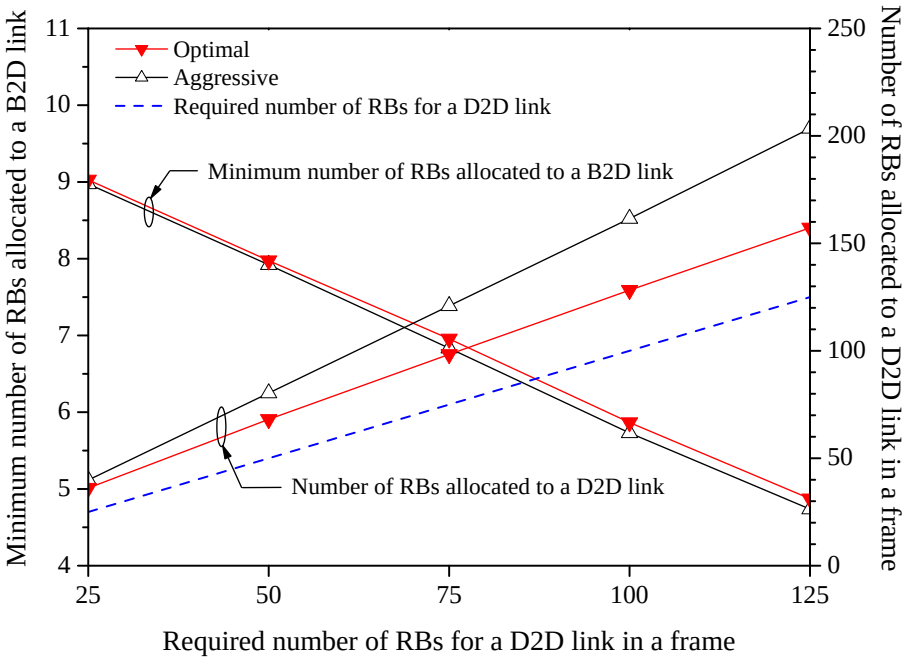

Fig. 4.8: Optimality gap of the aggressive scheme when there are ten D2D links in a cell.

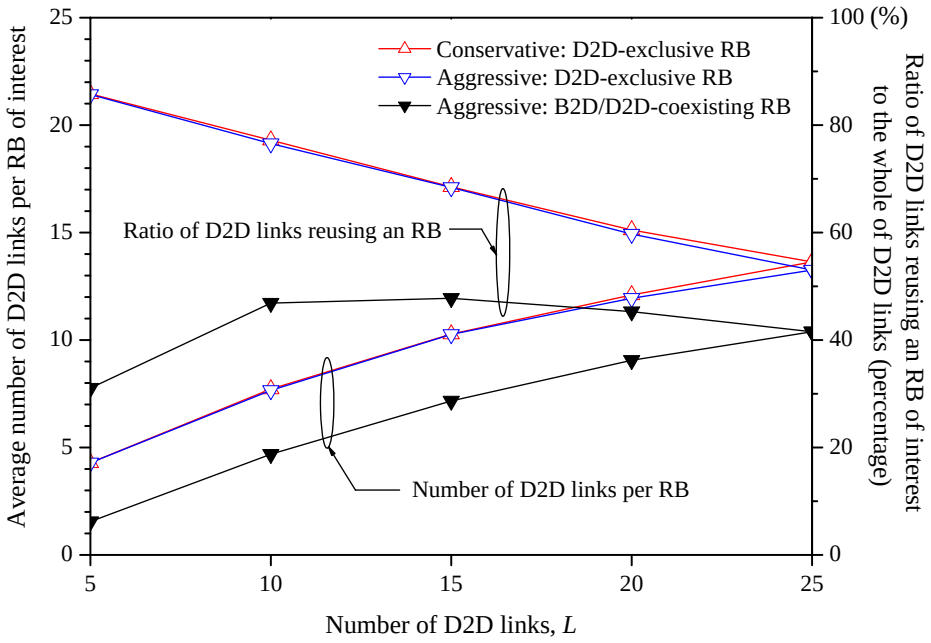

Fig. 4.9: Average number of D2D links per RB and proportion of D2D links reusing an RB on UL band.

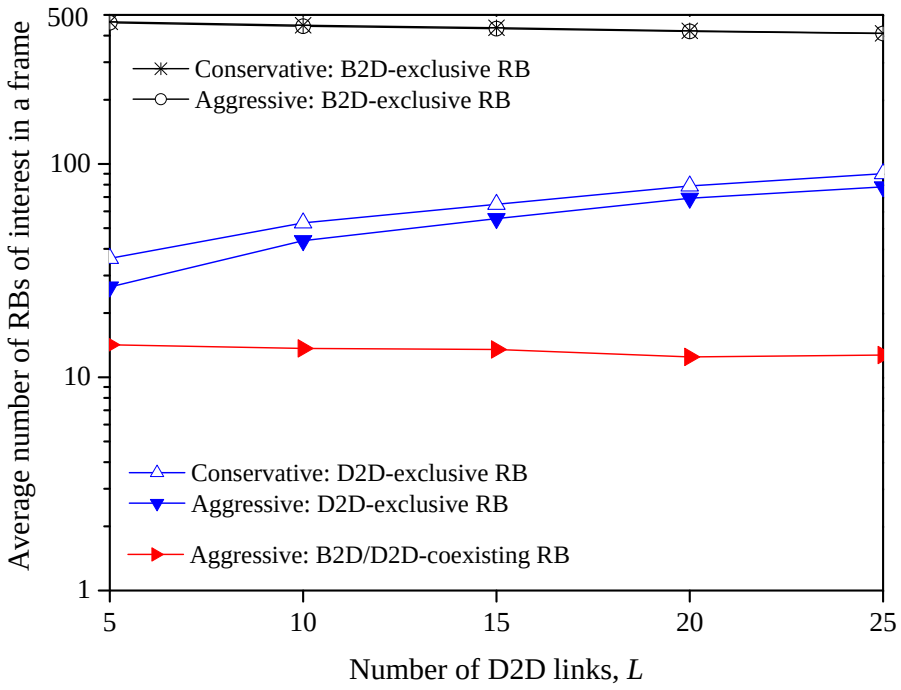

Fig. 4.10: Average numbers of D2D-exclusive RBs and B2D/D2D-coexisting RBs within a frame on UL band.

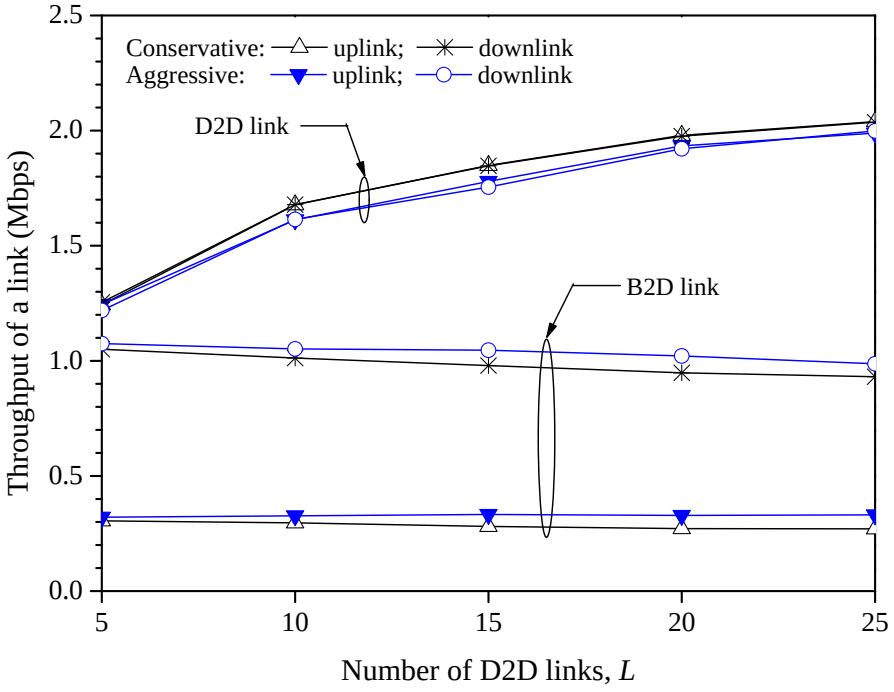

Fig. 4.11: Link throughput.

interference between them. Despite of that, even when $L = 25$, a D2D-exclusive RB is reused by about half of D2D links in a cell. In addition, Fig. 4.9 shows that an RB can be reused between a B2D link and multiple D2D links with aggressive reuse policy (e.g., about 10 D2D links on a B2D/D2D-coexisting RB when $L = 25$). Furthermore, as seen from Fig. 4.10, the conservative scheme produces many D2D-exclusive RBs within a frame and, with the aggressive policy, there are multiple B2D/D2D-coexisting RBs as well as D2D-exclusive RBs in a frame. This implies that the proposed schemes can enhance greatly the utilization of radio resource by exploiting efficiently the spatial reuse of RBs.

Fig. 4.11 shows the link throughputs of the proposed two schemes, where the link throughput means the average transmission rate of a link under the assumption of a full data buffer. As observed from the figure, since the aggressive scheme allows B2D links to reuse the RBs allocated to D2D links, it achieves the better performance than the conservative scheme, in the throughput of a B2D link. However, because of the interference from the B2D links using the same RBs, a D2D link has the lower throughput under the aggressive policy. On the other hand, it is obvious that a D2D link gets the higher throughput, because of its shorter length between transmitter and receiver, than a B2D link. Furthermore, a D2D link achieves almost the same throughput on both of uplink and downlink bands since a D2D link is built between two UEs.

Let us assess the influence that an RB reuse policy has on the performance. To this end, we compare in Fig. 4.12 the cell throughput of five schemes adopting different reuse policy, i.e., the proposed schemes with the conservative and aggressive reuse policies, the schemes in [25] and [26], and FlashLinQ scheme [23]. To concentrate on the influence of reuse policy, we apply the same power allocation policy to all of these schemes.

Before discussing the results in Fig. 4.12, we shortly describe the schemes in [25] and [26], and the FlashLinQ scheme. In all of these three schemes, B2D links have a priority over D2D links in selecting RBs and all RBs are first allocated to B2D links in a round robin manner. These schemes differ from each other in allocating the D2D links on RBs. The scheme in [25] allows only the simultaneous transmission of a B2D link and a D2D link on the same RB. For each B2D link, the scheme selects one D2D link which least interferes with the B2D link. The selected D2D link shares all the RBs allocated to the B2D link and is not considered any

more when the scheme selects a D2D link for the next B2D link. On the other hand, the scheme in [26] allocates, to each D2D link in decreasing order of its distance from the BS, the least number of RBs selected randomly for satisfying the required data rate of the D2D link.[1] For a fair comparison, we relax the constraint of the contiguous RB allocation in [26] so that an RB may be allocated simultaneously to a B2D link and one or more D2D links. The FlashLinQ scheme in [23] allows the distributed scheduling of D2D links by exchanging analog tone signals at start of each time slot. Randomized priorities are assigned to D2D links in each time slot. Links are scheduled in sequential order of priority, so as not to interfere with already scheduled links. For a fair comparison, we assume that the scheduling is done on per RB basis.

Let us examine Fig. 4.12. Since the schemes in [25] and [26] exploit full channel information for RB reuse, they accomplish the better performance than the FlashLinQ scheme using only the local information. Also, it is natural that the scheme in [26], where one or more D2D links can share the same RB with a B2D link, outperforms the scheme in [25] where only the reuse of at most one B2D link and one D2D link is allowed. On the other hand, because the scheme in [26] cannot efficiently find the feasible spatial reuse pattern because of heuristic approach, its throughput performance is worse than the proposed conservative RB allocation scheme that can almost optimally achieve simultaneous transmission of multiple D2D links on an RB (see Fig. 4.7). Furthermore, the proposed RB allocation scheme is able to obtain an additional throughput gain by allowing B2D/D2D-coexisting RBs with aggressive policy. This additional gain results from the increased flexibility of the

[1] For consistency, we calculate the required data rate of D2D link l as $N_l W_{\mathrm{RB}} \log_2(1 + \frac{-1.5}{ln(5 \times BER)}\gamma)$ where $\gamma = 9$ dB.

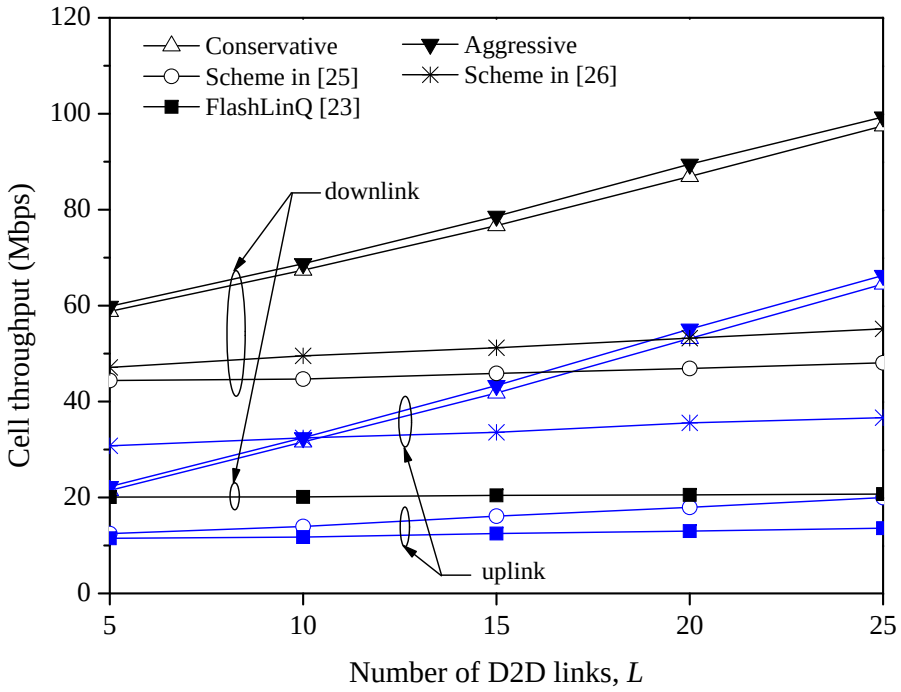

Fig. 4.12: Performance comparison in cell throughput.

spatial reuse of the RBs but it is not large, since the proportion of B2D/D2D-coexisting RBs in a frame is merely around 2–3 % as observed from Fig. 4.10. Accordingly, although the aggressive scheme enhances the spatial reuse of resource a little more, we recommend the conservative scheme when taking account of its lower computational complexity.

On the other hand, we can observe in Fig. 4.12 that the throughput performance of the proposed schemes is improved with more D2D links, since the number of D2D links on the same RB increases (see Fig. 4.9). However, the throughput improvement in the other three schemes is scarcely noticeable. The reason is as follows. All of these three schemes search the reusable RBs for D2D links after allocating all RBs to B2D links. Thus, when there are more D2D links in a cell, the total throughput of D2D links gets higher owing to the increased number of reused RBs, but the B2D throughput on reusable RBs gets lower because of the increased interference from D2D transmitters. By this combined effect, the throughput of an reused RB is not greatly higher than that of an RB allocated only to a B2D link, and this leads to the results of Fig. 4.12.

Next, we investigate in Table 4.2 how much resources are needed for control signaling. The signaling overhead is defined as the ratio of RBs used for control signaling to the total RBs. To calculate the signaling overhead, we adopt the control messages in the LTE system. For reporting the channel status of a link, a UE transmits a channel quality indicator (CQI). It is assumed that up to 6 CQIs can be transmitted in an RB without collision, the RB allocation information is delivered to UEs by using downlink control information (DCI), and two DCI formats are transmitted in an RB. As we can see from Table I, the proposed schemes require less signaling overhead than the other schemes. The proposed schemes with the

Tab. 4.2: Signaling overhead according to the number of D2D links

Number of D2D links	**Signaling overhead (%)**			
	Proposed schemes	**Scheme in [25]**	**Scheme in [26]**	**FlashLinQ**
$L = 5$	3.6	12.1	12.6	7.1
$L = 15$	3.8	29.7	33.4	14.3
$L = 25$	4.0	47.2	57.6	21.4

conservative and aggressive policies require the same amount of signaling overhead. Although the FlashLinQ scheme is a distributed scheme, it has more signaling overhead than the proposed schemes. This is because the scheduling is done on an RB basis, which requires D2D UEs to exchange analog tone signals in each RB.

Chapter 5. Conclusion

In this thesis, we have proposed two schemes for the cooperative communication and D2D communication, which can achieve the higher throughput while reducing signaling overhead.

To reduce signaling overhead in the cooperative communication, we have proposed an adaptive transmission scheme which decides the transmission rate and the transmission path in every frame based only on limited feedback. Three different feedback schemes according to the amount of feedback overhead are considered. Since the adaptive transmission scheme relies only on partial information about the channel states from limited CSI, we have designed the optimal scheme by using the POMDP framework. Although exact channel states cannot be known from limited feedback information, the cooperative communication network is able to determine the optimal transmission mode with the proposed scheme. Furthermore, we have also proposed a low-complexity myopic solution since solving a POMDP is computationally intensive.

The proposed resource management scheme for the D2D communication in cellular networks aims at a high network throughput of centralized scheme and a low signaling/computational overhead of distributed one. To do this, we have suggested a two-stage semi-distributed resource management framework where the first stage of the proposed framework is the long-term RB allocation performed by the BS and the second stage is the short-term link adaptation and scheduling accomplished by each D2D link and the BS in a distributed manner. In addition, we have formulated the RB allocation problem for the first stage with the goal of maximizing the spectrum efficiency and have proposed the algorithms with low complexity for efficiently solving the problem, under two different spatial reuse policies which

are called the conservative reuse and the aggressive reuse, respectively. With the conservative reuse policy, only the D2D links can be allocated simultaneously to the same RB, whereas with the aggressive policy the RB reuse is allowed between B2D and D2D links as well as among D2D links. Accordingly, the D2D links get the better transmission quality under the conservative policy than the aggressive one, but the network throughput can be improved further under the aggressive policy pursuing more spectrum reuse.

It is shown by simulation that the proposed adaptive transmission scheme outperforms even the full feedback scheme by minimizing feedback overhead and the proposed resource management scheme achieves the high throughput with low signaling overhead.

Bibliography

[1] D. Love, R. Heath, V. N. Lau, D. Gesbert, B. Rao, and M. Andrews, "An overview of limited feedback in wireless communication systems," *IEEE J. Sel. Areas in Commun.*, vol. 26, no. 8, pp. 1341–1365, Oct. 2008.

[2] C. Xiong, G. Y. Li, S. Zhang, Y. Chen, and S. Xu, "CSI feedback reduction for energy-efficient downlink OFDMA," in *Proc. IEEE WCNC 2012*, Apr. 2012, pp. 1135–1139.

[3] Y. Xiao and L. J. Cimini, "Impact of overhead on spectral efficiency of cooperative relaying," *IEEE Wireless Commun.*, vol. 12, no. 5, pp. 2228–2239, May 2013.

[4] X. Tao, X. Xu, and Q. Cui, "An overview of cooperative communications," *IEEE Commun. Mag.*, vol. 50, no. 6, pp. 65–71, June 2012.

[5] A. Nosratinia, T. E. Hunter, and A. Hedayat, "Cooperative communication in wireless networks," *IEEE Commun. Mag.*, vol. 42, no. 10, pp. 74–80, Oct. 2004.

[6] E. S. Altubaishi and X. Shen, "A generalized switching policy for incremental relaying with adaptive modulation," in *Proc. IEEE ICC 2010*, Cape Town, South Africa, May 2010, pp. 1–5.

[7] J. N. Laneman, D. N. C. Tse, and G. W. Wornell, "Cooperative diversity in wireless networks: Efficient protocols and outage behavior," *IEEE Trans. Inf. Theory*, vol. 50, no. 12, pp. 3062–3080, Dec. 2004.

[8] D. Panaitopol, P.-Y. Kong, C.-K. Tham, and A. Bagayoko, "A practical incremental relaying scheme with imperfect feedback for wireless networks," in *Proc. IEEE WCNC 2012*, Apr. 2012, pp. 1380–1385.

[9] A. H. Bastami and A. Olfat, "Selection relaying schemes for cooperative wireless networks with adaptive modulation," *IEEE Trans. Veh. Technol.*, vol. 60, no. 4, pp. 1539–1558, May 2011.

[10] A. James, A. S. Madhukumar, S. D. Tio, and E. Kurniawan, "Throughput optimization in cooperative communications based on incremental relaying," *IEEE Trans. Veh. Technol.*, vol. 60, no. 1, pp. 317–322, Jan. 2011.

[11] S. Ren, K. B. Letaief, and J. R. B. de Marca, "Outage reduction in cooperative networks with limited feedback," *IEEE Trans. Commun.*, vol. 58, no. 3, pp. 748–752, Mar. 2010.

[12] E. Karamad and R. Adve, "Channel quantization and bit allocation in multi-source multi-relay cooperative networks," in *Proc. IEEE CISS 2012*, Mar. 2012.

[13] K. Doppler, M. Rinne, C. Wijting, C. B. Ribeiro, and K. Hugl, "Device-to-device communication as an underlay to LTE-advanced networks," *IEEE Commun. Mag.*, vol. 47, no. 12, pp. 42–49, Dec. 2009.

[14] G. Fodor, E. Dahlman, G. Mildh, S. Parkvall, N. Reider, G. Miklos, and Z. Turanyi, "Design aspects of network assisted device-to-device communications," *IEEE Commun. Mag.*, vol. 50, no. 3, pp. 170–177, Mar. 2012.

[15] 3GPP TR 22.803, "Feasibility study for proximity services (ProSe) (Release 12)," Dec. 2012.

[16] D. Astely, E. Dahlman, G. Fodor, S. Parkvall, and J. Sachs, "LTE release 12 and beyond," *IEEE Commun. Mag.*, vol. 51, no. 7, pp. 154–160, June 2013.

[17] G. Fodor and N. Reider, "A distributed power control scheme for cellular network assisted D2D communications," in *Proc. IEEE GLOBECOM 2011*, Dec. 2011.

[18] H. Xing and S. Hakola, "The investigation of power control schemes for a device-to-device communication integrated into OFDMA cellular system," in *Proc. IEEE PIMRC 2010*, Sept. 2010, pp. 1775–1780.

[19] T. Peng, Q. Lu, H. Wang, S. Xu, and W. Wang, "Interference avoidance mechanisms in the hybrid cellular and device-to-device systems," in *Proc. IEEE PIMRC 2009*, Sept. 2009, pp. 617–621.

[20] S. Xu, H. Wang, T. Chen, Q. Huang, and T. Peng, "Effective interference cancellation scheme for device-to-device communication underlaying cellular networks," in *Proc. IEEE VTC-Fall 2010*, Sept. 2010.

[21] T. Chen, G. Charbit, and S. Hakola, "Time hopping for device-to-device communication in LTE cellular system," in *Proc. IEEE WCNC 2010*, Apr. 2010.

[22] H. S. Chae, J. Gu, B. Choi, and M. Y. Chung, "Radio resource allocation scheme for device-to-device communication in cellular networks using fractional frequency reuse," in *Proc. APCC 2011*, Oct. 2011, pp. 58–62.

[23] X. Wu, S. Tavildar, S. Shakkottai, T. Richardson, J. Li, R. Laroia, and A. Jovicic, "FlashLinQ: A synchronous distributed scheduler for peer-to-peer ad hoc networks," in *Proc. Allerton Conference on Communication 2010*, Sept. 2010, pp. 514–521.

[24] Z. Liu, T. Peng, S. Xiang, and W. Wang, "Mode selection for device-to-device (D2D) communication under LTE-advanced networks," in *Proc. IEEE ICC 2012*, June 2012, pp. 5563–5567.

[25] M. Zulhasnine, C. Huang, and A. Srinivasan, "Efficient resource allocation for device-to-device communication underlaying LTE network," in *Proc. IEEE WiMob 2010*, Oct. 2010, pp. 368–375.

[26] X. Zhu, S. Wen, G. Cao, X. Zhang, and D. Yang, "QoS-based resource allocation scheme for device-to-device (D2D) radio underlaying cellular networks," in *Proc. IEEE International Conference on Telecommunications (ICT) 2012*, Apr. 2012.

[27] T. Han, R. Yin, Y. Xu, and G. Yu, "Uplink channel reusing selection optimization for device-to-device communication underlaying cellular networks," in *Proc. IEEE PIMRC 2012*, Sept. 2012, pp. 559–564.

[28] R. Zhang, X. Cheng, L. Yang, and B. Jiao, "Interference-aware graph based resource sharing for device-to-device communciations underlaying cellular networks," in *Proc. IEEE WCNC 2013*, Apr. 2013.

[29] F. Wang, L. Song, Z. Han, Q. Zhao, and X. Wang, "Joint scheduling and resource allocation for device-to-device underlay communication," in *Proc. IEEE WCNC 2013*, Apr. 2013.

[30] M. Belleschi, G. Fodor, and A. Abrardo, "Performance analysis of a distributed resource allocation scheme for D2D communications," in *Proc. IEEE GLOBECOM Workshop Machine-to-Machine Commun.*, Dec. 2011, pp. 358–362.

[31] M.-H. Han, B.-G. Kim, and J.-W. Lee, "Subchannel and transmission mode scheduling for D2D communication in OFDMA networks," in *Proc. IEEE VTC-Fall 2012*, Sept. 2012.

[32] R. Moosavi and E. G. Larsson, "Reducing physical layer control signaling using mobile-assisted scheduling," *IEEE Trans. Wireless Commun.*, vol. 12, no. 1, pp. 368–379, Jan. 2013.

[33] M. Kang and K. S. Kim, "Performance analysis and optimization of best-M feedback for OFDMA systems," *IEEE Commun. Lett.*, vol. 16, no. 10, pp. 1648–1651, Oct. 2012.

[34] W. Wang, Z. Zhang, and H. Kayama, "Reducing signalling overhead by an enhanced differential codebook in multimode MIMO-OFDM systems," in *Proc. IEEE VTC-Fall 2010*, Sept. 2010.

[35] K. Ishihara, Y. Asai, R. Kudo, T. Ichikawa, and M. Mizoguchi, "Indoor experiments of real-time MU-MIMO with CSI feedback scheme for wireless LAN systems," in *Proc. IEEE VTC-Spring 2012*, May 2012.

[36] B. Zhou, L. Jiang, L. Zhang, C. He, S. Zhao, J. Zhining, and K. Zhao, "An optimal scheme for TDD beamforming systems with imperfect channel state information," in *Proc. IEEE VTC-Spring 2011*, May 2011.

[37] Y. Wu, Z. Tang, and E. G. Larsson, "Optimization of frame length in OFDMA systems taking into account the control signaling cost," in *Proc. IEEE VTC-Spring 2011*, May 2011.

[38] S. Yarkan and K. A. Qaraqe, "Analysis and characterization of the impact of frequency-selective interference on reporting period for next-generation wireless networks," *IEEE Trans. Veh. Technol.*, vol. 61, no. 8, pp. 3813–3819, Oct. 2012.

[39] S. Shrivastava and R. Vannithamby, "Group scheduling for improving VoIP capacity in IEEE 802.16e networks," in *Proc. IEEE VTC-Spring 200*, Apr. 2009.

[40] K. W. Choi, D. H. Lee, W. S. Jeon, and D. G. Jeong, "Group-based control scheme for machine type device-to-device communication," in *Proc. IEEE VTS APWCS 2012*, Aug. 2012.

[41] M. K. Kim and H. S. Lee, "Radio resource management for a two-hop OFDMA relay system in downlink," in *Proc. IEEE ISCC 2007*, July 2007, pp. 25–31.

[42] N. Yi, Y. Ma, and R. Tafazolli, "Joint rate adaptation and best-relay selection using limited feedback," *IEEE Trans. Wireless Commun.*, vol. 12, no. 6, pp. 2797–2805, June 2013.

[43] G. E. Monahan, "A survey of partially observable Markov decision processes: Theory, models, and algorithms," *Management Science*, vol. 28, no. 1, pp. 1–16, Jan. 1982.

[44] H. S. Wang and N. Moayeri, "Finite-state Markov channel – A useful model for radio communication channels," *IEEE Trans. Veh. Technol.*, vol. 44, no. 1, pp. 163–171, Feb. 1995.

[45] W. C. Jakes, *Microwave Mobile Communications.*, IEEE Press, 1974.

[46] I. Koutsoploulos and L. Tassiulas, "Optimal transmission rate control policies in a wireless link under partial state information," *IEEE Trans. Autom. Control*, vol. 55, no. 1, pp. 127–131, Jan. 2010.

[47] A. Goldsmith, *Wireless Communications.*, New York: Cambridge University Press, 2005.

[48] D. H. Lee, K. W. Choi, W. S. Jeon, and D. G. Jeong, "Resource allocation scheme for device-to-device communication for maximizing spatial reuse," in *Proc. IEEE WCNC 2013*, Apr. 2013.

[49] S. Hakola, T. Chen, J. Lehtomaki, and T. Koskela, "Device-to-device (D2D) communication in cellular network – Performance analysis of optimum and practical communication mode selection," in *Proc. IEEE WCNC 2010*, Apr. 2010.

[50] H. Fu and D. I. Kim, "Analysis of throughput and fairness with downlink scheduling in WCDMA networks," *IEEE Trans. Wireless Commun.*, vol. 5, no. 8, pp. 2164–2174, Aug. 2006.

[51] J. Yang and J. Y-T. Leung, "A generalization of the weighted set covering problem," *Naval Research Logistics*, vol. 52, no. 2, pp. 142–149, Mar. 2005.

[52] L. S. Lasdon, *Optimization Theory for Large Systems*, Mineola, NY: Dover, 2002.

[53] M. E. Lubbecke and J. Desrosiers, "Selected topics in column generation," *Operations Research*, vol. 53, no. 6, pp. 1007–1023, Dec. 2005.

[54] 3GPP TS 25.814, "Physical layer aspects for evolved universal terrestrial radio access (UTRA) (Release 7)," Sept. 2006.

[55] C. Xiao, Y. R. Zheng, and N. C. Beaulieu, "Novel sum-of-sinusoids simulation models for Rayleigh and Rician fading channels," *IEEE Trans. Wireless Commun.*, vol. 5, no. 12, pp. 3667–3679, Dec. 2006.

[56] A. J. Goldsmith and S.-G. Chua, "Variable-rate variable-power MQAM for fading channels," *IEEE Trans. Commun.*, vol. 45, no. 10, pp. 1218–1230, Oct. 1997.

초 록

무선통신망(wireless networks)은 무선 채널의 상태 변화에 따른 성능 저하를 줄이기 위해 링크 적응(link adaptation) 기술을 기본적으로 사용한다. 링크 적응 기술을 위해서는 채널 상태 정보를 추정하고 수집해야하기 때문에 이에 따른 신호전달 부하(signaling overhead)가 발생하게 된다. 본 논문에서는 무선통신망에서의 신호전달 부하를 줄이기 위한 두 가지 기법을 제안하였다. 먼저 협력 통신 네트워크(cooperative communication networks)에서의 적응적인 전송 기법을 제안하였다. 제안한 기법을 사용하는 협력 통신 네트워크는 ACK(positive acknowledgement)/NACK(negative ACK)와 같은 제한된 피드백 정보로부터 추정된 채널 상태에 기반을 두어 전송 속도를 조절하면서 릴레이(relay)의 사용 여부도 함께 결정한다. 제한된 피드백 정보는 실제 채널 상태에 대한 부분적인 정보만을 제공하기 때문에 제안하는 기법을 불확실성 마코브 의사 결정(partially observable Markov decision process)에 따라 설계하였다. 다음으로, 셀룰러 네트워크에서의 기기 간(D2D, device-to-device) 통신을 위한 자원 관리 기법을 제안하였다. 제안한 기법은 두 단계로 구성되고 준 분산적(semi-distributed)으로 동작한다. 첫 번째 단계에서는 중앙 집중적(centralized)으로 기지국이 자원 블록을 B2D(BS-to-user device) 링크와 D2D 링크에게 할당한다. 두 번째 단계에서는 분산적(distributed)으로 기지국은 B2D 링크에 할당된 자원 블록들을 사용하여 전송 스케줄을 결정(scheduling)하고, 각 D2D 링크의 제 1 사용자 기기(primary user device)는 해당 D2D 링크에 할당된 자원 블록들에서의 링크 적응을 수행한다. 이러한 자원 관리 구조는 중앙 집중적 기법처럼 높은 네트워크 용량을 달성할 뿐 아니라 분산적 기법처럼 낮은 신호전달 및 계산(computational) 부하를 필요로 한다. 본 논문에서는 제안한 자원 관리 구조에서 주파수 자원 효율을 최대화하는 자원 블록 할당 문제들을 두

가지 서로 다른 자원 할당 정책에 대하여 만들고 이 문제들을 풀기 위해 탐욕(greedy) 알고리즘과 열 추가 기반(column generation-based) 알고리즘을 제안하였다. 또한 시뮬레이션을 통해 제안하는 기법들이 설계 목표를 달성하고 기존의 기법보다 높은 성능을 보이면서도 신호전달 부하를 줄일 수 있음을 보였다.

주요어: 신호전달 부하, 협력 통신, 기기간 통신, 선택적 릴레이, 적응 변조 및 코딩, 자원 관리
학　번: 2007-30232